ESAIM: M2AN 58 (2024) 857–880
https://doi.org/10.1051/m2an/2024022

ESAIM: Mathematical Modelling and Numerical Analysis
www.esaim-m2an.org

AN EXACT IN TIME FOURIER PSEUDOSPECTRAL METHOD WITH MULTIPLE CONSERVATION LAWS FOR THREE-DIMENSIONAL MAXWELL'S EQUATIONS

Bin Wang and Yaolin Jiang*

Abstract. Maxwell's equations describe the propagation of electromagnetic waves and are therefore fundamental to understanding many problems encountered in the study of antennas and electromagnetics. The aim of this paper is to propose and analyse an efficient fully discrete scheme for solving three-dimensional Maxwell's equations. This is accomplished by combining Fourier pseudospectral methods in space and exact formulation in time. Fast computation is efficiently implemented in the scheme by using the matrix diagonalisation method and fast Fourier transform algorithm which are well known in scientific computations. An optimal error estimate which is not encumbered by the CFL condition is established and the resulting scheme is proved to be of spectral accuracy in space and exact in time. Furthermore, the scheme is shown to have multiple conservation laws including discrete energy, helicity, momentum, symplecticity, and divergence-free field conservations. All the theoretical results of the accuracy and conservations are numerically illustrated by two numerical tests.

Mathematics Subject Classification. 65M12, 65M15, 65M70.

Received September 15, 2023. Accepted March 20, 2024.

1. Introduction

The Maxwell's equations are well-known to be the fundamental laws in electromagnetism and they describe the propagation and scattering of electromagnetic waves. They play a crucial role in a wide variety of applications in science and engineering such as wireless engineering, antennas, microwave circuits, photonic cristals, radio-frequency, aircraft radar, integrated optical circuits, waveguides, and interferometers. This paper is devoted to the three-dimensional Maxwell's equations in an isotropic, homogeneous, and lossless medium which are expressed in the following coupled form (see [29])

$$\begin{cases} \dfrac{\partial \mathbf{H}}{\partial t} = -\dfrac{1}{\mu}\mathbf{curl}\ \mathbf{E}, & \dfrac{\partial \mathbf{E}}{\partial t} = \dfrac{1}{\varepsilon}\mathbf{curl}\ \mathbf{H}, \quad \textbf{(curl-equations)} & (1.1a) \\ \nabla\cdot(\varepsilon\mathbf{E}) = 0, & \nabla\cdot(\mu\mathbf{H}) = 0, \quad \textbf{(div-equations)} & (1.1b) \end{cases}$$

where

$$\mathbf{H}(x,y,z,t) = (H_x(x,y,z,t), H_y(x,y,z,t), H_z(x,y,z,t))^{\intercal} : \Omega \times [0, t_{\text{end}}] \to \mathbb{R}^3$$

Keywords and phrases. Maxwell's equations, exact in time Fourier pseudospectral method, Duhamel's formula, structure-preserving algorithms, convergence.

School of Mathematics and Statistics, Xi'an Jiaotong University, Xi'an, Shannxi 710049, P.R. China.
*Corresponding author: yljiang@mail.xjtu.edu.cn.

stands for magnetic field intensity,

$$\mathbf{E}(x,y,z,t) = (E_x(x,y,z,t), E_y(x,y,z,t), E_z(x,y,z,t))^\intercal : \Omega \times [0, t_{\text{end}}] \to \mathbb{R}^3$$

represents electric field intensity, and μ and ε denote the magnetic permeability and electric permittivity, respectively. In this paper, the equations (1.1) and their initial values

$$\mathbf{H}_0(x,y,z) = \mathbf{H}(x,y,z,0), \qquad \mathbf{E}_0(x,y,z) = \mathbf{E}(x,y,z,0), \tag{1.2}$$

are considered on the cuboid space domain $\Omega = [x_L, x_R] \times [y_L, y_R] \times [z_L, z_R]$ and periodic boundary conditions are required on the domain $\partial\Omega \times [0, t_{\text{end}}]$. It is well known that the solutions of Maxwell's equations (1.1) are unique and smooth for all time if the initial data (1.2) are suitably smooth [29]. The **div-equations** (1.1b) can be derived from the **curl-equations** (1.1a) by taking divergence, and they hold automatically if $\mathbf{H}_0$ and $\mathbf{E}_0$ are divergence-free.

Due to the great importance and diversity of applications, Maxwell's equations have been researched for more than 150 years and there has been a great interest in their numerical analysis in the last couple of decades. Various numerical methods have been investigated for the Maxwell's equations. The first kind of scheme was the finite-difference time domain (FDTD) method which was firstly proposed by Yee in [52], and further developed and analysed in [34,39,42,44,45,54]. However, these Yee-based FDTD methods require very small temporal step-size to ensure their stability. In order to improve the efficiency, the alternating direction implicit (ADI) technique was proposed and some unconditionally stable ADI-FDTD schemes were formulated in [15, 27, 28, 37, 52, 55]. Besides finite-difference space discretization, other space discretization techniques have also become common such as discontinuous Galerkin (dG) methods [9,10,12,33,35,53] or the Fourier pseudo-spectral method [31]. It should be noted that although the finite-difference or discontinuous Galerkin methods are less accurate or maybe not structure preserving, they are applicable to more general boundary conditions which is a superiority for the scientific computing of Maxwell's equations. Concerning the schemes of time integrations, some time methods are applied to the spatially discretised Maxwell's equations such as the explicit method [16], Verlet method [14], Runge–Kutta (RK) methods [22, 23], splitting methods [25, 47], low-storage RK schemes [11], multiscale methods [19, 26], and exponential methods [38, 51].

It is noted that the above mentioned publications are devoted to accuracy and they do not pay attention to structure preservation. In recent years, due to the superior properties in long time integrations over traditional numerical algorithms, structure-preserving methods have been shown to be very powerful and have gained remarkable success [17]. For the Maxwell's equations (1.1), they admit many physical invariants: energy conservation laws, symplectic conservation laws, helicity conservation laws, momentum conservation laws and divergence-free fields. These invariants are very important in the long time propagation of the electromagnetic waves [45].

To present these physical invariants, we rewrite the two **curl-equations** (1.1a) as a bi-Hamiltonian system [32] which reads

$$\frac{\partial}{\partial t}\begin{pmatrix}\mathbf{H}\\ \mathbf{E}\end{pmatrix} = \begin{pmatrix}\mathbf{0} & -\frac{\mathbf{curl}}{\varepsilon\mu}\\ \frac{\mathbf{curl}}{\varepsilon\mu} & \mathbf{0}\end{pmatrix}\begin{pmatrix}\frac{\delta\mathcal{H}}{\delta\mathbf{H}}\\ \frac{\delta\mathcal{H}}{\delta\mathbf{E}}\end{pmatrix},$$

where the quadratic Hamiltonian functional is $\mathcal{H} = \frac{1}{2}\int_\Omega (\varepsilon|\mathbf{E}|^2 + \mu|\mathbf{H}|^2)\,\mathrm{d}x\,\mathrm{d}y\,\mathrm{d}z$ with the Euclidean norm $|\cdot|$. The solutions $\mathbf{E}, \mathbf{H}$ satisfy the following energy conservation laws (ECLs) for $w = x, y$ or z [3, 7]

$$\begin{aligned}
&\frac{\mathrm{d}}{\mathrm{d}t}\mathcal{E}_1^{\text{exact}}(t) = 0, \quad \mathcal{E}_1^{\text{exact}}(t) := \mathcal{H} = \frac{1}{2}\int_\Omega \left(\varepsilon|\mathbf{E}|^2 + \mu|\mathbf{H}|^2\right)\mathrm{d}x\,\mathrm{d}y\,\mathrm{d}z,\\
&\frac{\mathrm{d}}{\mathrm{d}t}\mathcal{E}_2^{\text{exact}}(t) = 0, \quad \mathcal{E}_2^{\text{exact}}(t) := \frac{1}{2}\int_\Omega \left(\varepsilon|\partial_t\mathbf{E}|^2 + \mu|\partial_t\mathbf{H}|^2\right)\mathrm{d}x\,\mathrm{d}y\,\mathrm{d}z,\\
&\frac{\mathrm{d}}{\mathrm{d}t}\mathcal{E}_3^{\text{exact}}(t) = 0, \quad \mathcal{E}_3^{\text{exact}}(t) := \frac{1}{2}\int_\Omega \left(\varepsilon|\partial_w\mathbf{E}|^2 + \mu|\partial_w\mathbf{H}|^2\right)\mathrm{d}x\,\mathrm{d}y\,\mathrm{d}z,
\end{aligned}$$

$$\frac{\mathrm{d}}{\mathrm{d}t}\mathcal{E}_4^{\text{exact}}(t)=0,\quad \mathcal{E}_4^{\text{exact}}(t):=\frac{1}{2}\int_\Omega\Big(\varepsilon\big|\partial_{tw}^2\mathbf{E}\big|^2+\mu\big|\partial_{tw}^2\mathbf{H}\big|^2\Big)\,\mathrm{d}x\,\mathrm{d}y\,\mathrm{d}z. \tag{1.3}$$

With the Hamiltonian formulation, the Maxwell's equations (1.1) also satisfy the symplectic conservation law [44]

$$\frac{\mathrm{d}}{\mathrm{d}t}\int_\Omega(\mathrm{d}E_x\wedge\mathrm{d}H_x+\mathrm{d}E_y\wedge\mathrm{d}H_y+\mathrm{d}E_z\wedge\mathrm{d}H_z)\,\mathrm{d}x\,\mathrm{d}y\,\mathrm{d}z=0, \tag{1.4}$$

the helicity conservation laws [4]

$$\begin{aligned}
&\frac{\mathrm{d}}{\mathrm{d}t}\mathcal{H}_1^{\text{exact}}(t)=0,\quad \mathcal{H}_1^{\text{exact}}(t):=\int_\Omega\left(\frac{\mathbf{E}^\intercal(\mathbf{curl}\ \mathbf{E})}{2\mu}+\frac{\mathbf{H}^\intercal(\mathbf{curl}\ \mathbf{H})}{2\varepsilon}\right)\mathrm{d}x\,\mathrm{d}y\,\mathrm{d}z,\\
&\frac{\mathrm{d}}{\mathrm{d}t}\mathcal{H}_2^{\text{exact}}(t)=0,\quad \mathcal{H}_2^{\text{exact}}(t):=\int_\Omega\left(\frac{(\partial_t\mathbf{E})^\intercal(\mathbf{curl}\ \partial_t\mathbf{E})}{2\mu}+\frac{(\partial_t\mathbf{H})^\intercal(\mathbf{curl}\ \partial_t\mathbf{H})}{2\varepsilon}\right)\mathrm{d}x\,\mathrm{d}y\,\mathrm{d}z,
\end{aligned} \tag{1.5}$$

and the momentum conservation laws [4]

$$\begin{aligned}
&\frac{\mathrm{d}}{\mathrm{d}t}\mathcal{M}_1^{\text{exact}}(t)=0,\quad \mathcal{M}_1^{\text{exact}}(t):=\int_\Omega(\mathbf{H}^\intercal\partial_w\mathbf{E})\,\mathrm{d}x\,\mathrm{d}y\,\mathrm{d}z,\quad \text{where}\ \ w=x,y,z,\\
&\frac{\mathrm{d}}{\mathrm{d}t}\mathcal{M}_2^{\text{exact}}(t)=0,\quad \mathcal{M}_2^{\text{exact}}(t):=\int_\Omega(\mathbf{E}^\intercal\partial_w\mathbf{H})\,\mathrm{d}x\,\mathrm{d}y\,\mathrm{d}z,\quad \text{where}\ \ w=x,y,z.
\end{aligned} \tag{1.6}$$

For Maxwell's equations, these physical invariants are important which are desirable to be preserved by a numerical scheme in the discrete sense [17, 50]. Thus, structure-preserving algorithms have received much attention in the numerical analysis of Maxwell's equations since they can inherit the original invariants as much as possible. Concerning the structure-preserving algorithms of Maxwell's equations, three categories have been received much attention in recent years: sympletic methods, divergence-free methods and energy-preserving methods.

There has been a great interest in solving Maxwell's equations by using symplectic methods (see, *e.g.*, [2, 20, 28, 41, 43, 44, 56]), which can preserve the symplectic conservation law (1.4) of the equations. In order to make the numerical solution satisfy the div-equations (1.1b), divergence-free methods were analised (see, *e.g.*, [8, 36]). Another important component of the structure-preserving methods is the energy-preserving method. A kind of energy-conserved splitting method was proposed in [6] for two dimensional Maxwell's equations and in [7] for the three dimensional case. Some energy preserving and unconditionally stable splitting schemes [3, 13, 27, 28, 30] were further proposed. However, most of these energy-conserved splitting schemes have only second order accuracy in both time and space at most. In order to improve the accuracy, another energy-conserved scheme with fourth order accuracy in time was given in [4].

There is no doubt that the idea to make use of structure-preserving algorithms for Maxwell's equations is by no means new, but there are still many key issues in such kind of algorithms which remain to be well researched. In this paper, a kind of scheme with high accuracy, low cost and multiple conservation laws is derived and analised for Maxwell's equations. The main contributions of this paper are as follows.

(a) Among all the existing structure-preserving methods for Maxwell's equations, explicit methods usually suffer from step size restrictions due to stability requirements (CFL condition) and implicit methods can use larger time steps at the cost of solving linear or even nonlinear systems. Meanwhile, all the methods have limited accuracy (up to order four) in time. In this paper, we will formulate a kind of explicit fully discrete scheme for (1.1) which is not encumbered by the CFL condition (any large time step-size is acceptable). An optimal error is established and the new scheme is shown to have spectral accuracy in space and exact in time.

(b) Usually the structure-preserving algorithms of Maxwell's equations can preserve some physical invariants. The new scheme proposed in this paper can simultaneously preserve the energy, symplecticity, helicity, momentum and divergence-free fields conservation laws.

(c) For all the energy-preserving methods of Maxwell's equations, they are implicit and the iterative procedure is needed. However, the fully discrete scheme proposed in this paper is explicit and exact in time, and thus its computational cost is very low. Meanwhile, the scheme can be implemented by using the matrix diagonalisation method and Fast Fourier Transform (FFT) algorithm which are very efficient in scientific computing.

(d) The proposed scheme needs the regularity $C^1(0, t_{\text{end}}; [H_p^r(\Omega)]^3)$ with $r > 3/2$ of $\mathbf{H}$ and $\mathbf{E}$ to get the spectral accuracy in space and infinite-order accuracy in time, which is lower than those methods (spectral accuracy in space and second or fourth-order accuracy in time) required in the publications (see, *e.g.*, [2–4]).

The rest of the paper is organised as follows. In Section 2, we present the formulation of the fully discrete scheme and discuss its cost. The convergence analysis is done in Section 3. Section 4 presents the conservative properties of the proposed scheme. Two numerical experiments are displayed in Section 5 and the results demonstrate the high accuracy and exact conservation laws of the proposed scheme.

2. Description of the fully discrete scheme

2.1. Analytical framework

We begin this subsection with presenting some notations. For a set $K \subset \Omega$ and the vectors fields $\mathbf{U}, \widetilde{\mathbf{U}}, \mathbf{V}, \widetilde{\mathbf{V}} : K \to \mathbb{R}^3$ the $L^2(K)$-inner product is denoted by $\langle \mathbf{U}, \widetilde{\mathbf{U}} \rangle_K = \int_K \mathbf{U} \cdot \widetilde{\mathbf{U}} \, \mathrm{d}x \, \mathrm{d}y \, \mathrm{d}z$ and for $F \subset \partial K$ we denote $\langle \mathbf{U}, \widetilde{\mathbf{U}} \rangle_F = \int_F \mathbf{U}|_F \cdot \widetilde{\mathbf{U}}|_F \, \mathrm{d}\sigma$. Denoting by $\mathbf{u} = (\mathbf{U}, \mathbf{V})$ and $\widehat{\mathbf{u}} = (\widehat{\mathbf{U}}, \widehat{\mathbf{V}})$, the weighted inner products are given by

$$\left\langle \mathbf{U}, \widetilde{\mathbf{U}} \right\rangle_{\alpha,K} = \left\langle \alpha \mathbf{U}, \widetilde{\mathbf{U}} \right\rangle_K, \quad \langle \mathbf{u}, \widetilde{\mathbf{u}} \rangle_{\alpha\times\beta,K} = \left\langle \mathbf{U}, \widetilde{\mathbf{U}} \right\rangle_{\alpha,K} + \left\langle \mathbf{V}, \widetilde{\mathbf{V}} \right\rangle_{\beta,K}$$

for the positive weight functions $\alpha, \beta : \Omega \to \mathbb{R}^+$. The corresponding norms are immediately obtained as $\|\mathbf{U}\|_\alpha^2 = \langle \mathbf{U}, \mathbf{U} \rangle_{\alpha,K}$ and $\|\mathbf{u}\|_{\alpha\times\beta}^2 = \|\mathbf{U}\|_\alpha^2 + \|\mathbf{V}\|_\beta^2$.

The two **curl-equations** (1.1a) can be written as an abstract Cauchy problem

$$\frac{\partial}{\partial t} \begin{pmatrix} \sqrt{\mu}\mathbf{H} \\ \sqrt{\varepsilon}\mathbf{E} \end{pmatrix} = \mathcal{C} \begin{pmatrix} \sqrt{\mu}\mathbf{H} \\ \sqrt{\varepsilon}\mathbf{E} \end{pmatrix}, \tag{2.1}$$

where $\mathcal{C} = \begin{pmatrix} \mathbf{0} & -\mathcal{C}_{\mathbf{E}} \\ \mathcal{C}_{\mathbf{H}} & \mathbf{0} \end{pmatrix} = \begin{pmatrix} \mathbf{0} & -\frac{\mathbf{curl}}{\sqrt{\mu\varepsilon}} \\ \frac{\mathbf{curl}}{\sqrt{\mu\varepsilon}} & \mathbf{0} \end{pmatrix}$ is the Maxwell operator. For the **curl** operator, its graph space is given by

$$H(\mathbf{curl}, \Omega) = \left\{ \mathbf{U} \in L^2(\Omega)^3 \mid \mathbf{curl}\mathbf{U} \in L^2(\Omega)^3 \right\},$$

which is endowed with the inner product

$$\langle \mathbf{U}, \mathbf{V} \rangle_{H(\mathbf{curl},\Omega)} = \langle \mathbf{U}, \mathbf{V} \rangle_\Omega + \langle \mathbf{curl}\mathbf{U}, \mathbf{curl}\mathbf{V} \rangle_\Omega$$

for all $\mathbf{U}, \mathbf{V} \in H(\mathbf{curl}, \Omega)$ and the associated norm given by $\|\mathbf{U}\|_{H(\mathbf{curl},\Omega)}^2 = \langle \mathbf{U}, \mathbf{U} \rangle_{H(\mathbf{curl},\Omega)}$. Denote $H_0(\mathbf{curl}, \Omega)$ the closure of

$$C_0^\infty(\Omega)^3 = \{ v \in C^\infty(\Omega) | \text{supp}(v) \subset \Omega \text{ is compact} \}^3$$

with respect to the norm $\|\cdot\|_{H(\mathbf{curl},\Omega)}$. With these notations, it is well known that the Maxwell operator $\mathcal{C}$ is skew-adjoint w.r.t. $\langle \cdot, \cdot \rangle_{\alpha\times\beta,\Omega}$ [25], *i.e.*,

$$\langle \mathcal{C}_{\mathbf{H}}\mathbf{H}, \mathbf{E} \rangle_{\varepsilon,\Omega} = \langle \mathbf{H}, \mathcal{C}_{\mathbf{E}}\mathbf{E} \rangle_{\mu,\Omega}$$

for $\mathbf{H} \in D(\mathcal{C}_{\mathbf{H}})$ and $\mathbf{E} \in D(\mathcal{C}_{\mathbf{E}})$. Meanwhile, the Maxwell operator $\mathcal{C}$ with domain $D(\mathcal{C}) = D(\mathcal{C}_{\mathbf{E}}) \times D(\mathcal{C}_{\mathbf{H}}) = H(\mathbf{curl}, \Omega) \times H_0(\mathbf{curl}, \Omega)$ generates a unitary C_0-group $e^{t\mathcal{C}}$ [25] on a Hilbert space X.

Based on the above results, the well-posedness of Maxwell's equations can be derived by Stone's theorem. If the initial value $(\mathbf{H}_0, \mathbf{E}_0) \in D(\mathcal{C})$, the two curl-equations (1.1a) have a unique solution in $C^1(0, t_{\text{end}}; X) \cap C(0, t_{\text{end}}; D(\mathcal{C}))$ [25] which can be given by $\begin{pmatrix} \sqrt{\mu}\mathbf{H}(t) \\ \sqrt{\varepsilon}\mathbf{E}(t) \end{pmatrix} = e^{t\mathcal{C}} \begin{pmatrix} \sqrt{\mu}\mathbf{H}_0 \\ \sqrt{\varepsilon}\mathbf{E}_0 \end{pmatrix}$. According to this formula and the unitarity of $e^{t\mathcal{C}}$, the solution is bounded by

$$\|(\mathbf{H}, \mathbf{E})\|_{\mu\times\varepsilon,\Omega} \le \|(\mathbf{H}_0, \mathbf{E}_0)\|_{\mu\times\varepsilon,\Omega}. \tag{2.2}$$

If these solutions $\mathbf{H}, \mathbf{E}$ are required to be smooth enough and the initial values (1.2) satisfy the two **div-equations** (1.1b), *i.e.*, $\nabla \cdot (\varepsilon\mathbf{E}_0) = 0,\ \nabla \cdot (\varepsilon\mathbf{H}_0) = 0$, then the two div-equations (1.1b) hold true for $\mathbf{H}, \mathbf{E}$ at any $t \ge 0$. In the remaining parts of this section, the numerical scheme will be derived for the abstract Cauchy problem (2.1). Then, in the next section we will show the fact that the proposed numerical solution satisfies the two **div-equations** (1.1b).

2.2. Spatial discretisation

To achieve high order accuracy in treating the space, the Fourier pseudo-spectral method is a very good discretisation. With this we are hopeful of obtaining high order accuracy and be implemented by the Fast Fourier Transform (FFT) algorithm [31, 40, 46].

For the three-dimensional domain $\Omega = [x_L, x_R] \times [y_L, y_R] \times [z_L, z_R]$, define a series of collocation points $x_j = x_L + (j-1)h_x,\ y_k = y_L + (k-1)h_y,\ z_l = z_L + (l-1)h_z,\ j = 1, 2, \ldots, N_x,\ k = 1, 2, \ldots, N_y,\ l = 1, 2, \ldots, N_z$, where $h_x = (x_R - x_L)/N_x,\ h_y = (y_R - y_L)/N_y,\ h_z = (z_R - z_L)/N_z$ with even integers N_x, N_y, and N_z. Denote the time step-size by $\Delta t = t_{\text{end}}/N_t$ for some integer N_t and let $t_n = n\Delta t$. The value of the function $E(x, y, z, t)$ at the node (x_j, y_k, z_l, t_n) is denoted by $E^n_{j,k,l}$.

Denote a three-dimensional smooth function defined on $\Omega \times [0, t_{\text{end}}]$ by $U(x, y, z, t)$. The interpolation space of this function is considered as

$$\mathcal{S}_{N_S} = \text{span}\{g_j(x)g_k(y)g_l(z),\quad j = 1, 2, \ldots, N_x,\ k = 1, 2, \ldots, N_y,\ l = 1, 2, \ldots, N_z\},$$

where $N_S = N_x N_y N_z$ and $g_j(x), g_k(y), g_l(z)$ are trigonometric polynomials of degree $N_x/2, N_y/2, N_z/2$, given respectively by

$$g_j(x) = \frac{1}{N_x} {\sum_{|m|\le N_x/2}}' e^{im\nu_x(x-x_j)},\quad g_k(y) = \frac{1}{N_y} {\sum_{|m|\le N_y/2}}' e^{im\nu_y(y-y_k)},\quad g_l(z) = \frac{1}{N_z} {\sum_{|m|\le N_z/2}}' e^{im\nu_z(z-z_l)}.$$

Here $i = \sqrt{-1}$ and the prime indicates that the first and last terms in the summation are taken with the factor $1/2$, and $\nu_w = \frac{2\pi}{w_R - w_L}$ for $w = x, y, z$. Interpolating $U(x, y, z, t)$ at collocation points (x_j, y_k, z_l) gives

$$U(x, y, z, t) \approx \mathcal{I}_{N_S} U(x, y, z, t) = \sum_{j=1}^{N_x}\sum_{k=1}^{N_y}\sum_{l=1}^{N_z} U_{j,k,l}(t) g_j(x) g_k(y) g_l(z),$$

where $U_{j,k,l}(t) = U(x_j, y_k, z_l, t)$ and its vector form is denoted by

$$\mathbf{U} = \big(U_{1,1,1}, U_{2,1,1}, \ldots, U_{N_x,1,1}, U_{1,2,1}, U_{2,2,1}, \ldots, U_{N_x,2,1}, \ldots, U_{1,N_y,N_z}, U_{2,N_y,N_z}, \ldots, U_{N_x,N_y,N_z}\big)^{\intercal}.$$

Consider the following trigonometric polynomials as an approximation for the solution of (2.1)

$$\mathcal{I}_{N_S}\mathbf{H}^{\mathcal{F}} = \big(\mathcal{I}_{N_S}H_x^{\mathcal{F}}, \mathcal{I}_{N_S}H_y^{\mathcal{F}}, \mathcal{I}_{N_S}H_z^{\mathcal{F}}\big)^{\intercal},\quad \mathcal{I}_{N_S}\mathbf{E}^{\mathcal{F}} = \big(\mathcal{I}_{N_S}E_x^{\mathcal{F}}, \mathcal{I}_{N_S}E_y^{\mathcal{F}}, \mathcal{I}_{N_S}E_z^{\mathcal{F}}\big)^{\intercal}, \tag{2.3}$$

which is required to satisfy

$$\frac{\partial}{\partial t}\begin{pmatrix} \sqrt{\mu}\mathcal{I}_{N_S}\mathbf{H}^{\mathcal{F}} \\ \sqrt{\varepsilon}\mathcal{I}_{N_S}\mathbf{E}^{\mathcal{F}} \end{pmatrix} = \mathcal{C}\begin{pmatrix} \sqrt{\mu}\mathcal{I}_{N_S}\mathbf{H}^{\mathcal{F}} \\ \sqrt{\varepsilon}\mathcal{I}_{N_S}\mathbf{E}^{\mathcal{F}} \end{pmatrix}.$$

In order to calculate $\mathbf{curl}(\mathcal{I}_{N_S}\mathbf{E}^{\mathcal{F}})$, we take a partial derivative with respect to x and evaluate the resulting expression at collocation points (x_j, y_k, z_l):

$$\begin{aligned}\frac{\partial}{\partial x}\mathcal{I}_{N_S}E_x^{\mathcal{F}}(x_j,y_k,z_l) &= \sum_{j'=1}^{N_x}\sum_{k'=1}^{N_y}\sum_{l'=1}^{N_z} E_{x,j',k',l'}^{\mathcal{F}}(t)\frac{d}{dx}g_{j'}(x_j)g_{k'}(y_k)g_{l'}(z_l)\\ &= \big[(I_{N_z}\otimes I_{N_y}\otimes D_x)\mathbf{E}_x^{\mathcal{F}}\big]_{N_xN_y(l-1)+N_x(k-1)+j},\end{aligned}$$

where $\otimes$ is the Kronecker product, I_{N_w} is the identity matrix of dimension $N_w \times N_w$,

$$\mathbf{E}_x^{\mathcal{F}} = \Big(E_{x,1,1,1}^{\mathcal{F}},\dots,E_{x,N_x,1,1}^{\mathcal{F}},E_{x,1,2,1}^{\mathcal{F}},\dots,E_{x,N_x,2,1}^{\mathcal{F}},\dots,E_{x,1,N_y,N_z}^{\mathcal{F}},\dots,E_{x,N_x,N_y,N_z}^{\mathcal{F}}\Big)^{\intercal},$$

and the spectral differential matrix is explicitly given by

$$(D_w)_{j,l} = \frac{1}{2}\nu_w(-1)^{j+l}\cot(\nu_w(w_j-w_l)/2)$$

for $j \neq l$ and other elements are zero with $j,l = 1,2,\dots,N_w$ and $w = x,y,z$. Similarly, one has

$$\frac{\partial}{\partial y}\mathcal{I}_{N_S}E_x^{\mathcal{F}}(x_j,y_k,z_l) = \big[(I_{N_z}\otimes D_y\otimes I_{N_x})\mathbf{E}_x^{\mathcal{F}}\big]_{N_xN_y(l-1)+N_x(k-1)+j}$$

and

$$\frac{\partial}{\partial z}\mathcal{I}_{N_S}E_x^{\mathcal{F}}(x_j,y_k,z_l) = \big[(D_z\otimes I_{N_y}\otimes I_{N_x})\mathbf{E}_x^{\mathcal{F}}\big]_{N_xN_y(l-1)+N_x(k-1)+j}.$$

Based on the above results and with the notations $\widetilde{\mathbf{H}} = (\mathbf{H}_x^{\mathcal{F}},\mathbf{H}_y^{\mathcal{F}},\mathbf{H}_z^{\mathcal{F}})^{\intercal}$, $\widetilde{\mathbf{E}} = (\mathbf{E}_x^{\mathcal{F}},\mathbf{E}_y^{\mathcal{F}},\mathbf{E}_z^{\mathcal{F}})^{\intercal}$, the following ordinary differential equations are obtained

$$\frac{\mathrm{d}}{\mathrm{d}t}\begin{pmatrix}\sqrt{\mu}\widetilde{\mathbf{H}}\\ \sqrt{\varepsilon}\widetilde{\mathbf{E}}\end{pmatrix} = \frac{1}{\sqrt{\mu\varepsilon}}\begin{pmatrix}\mathbf{0} & -\mathbf{D}\\ \mathbf{D} & \mathbf{0}\end{pmatrix}\begin{pmatrix}\sqrt{\mu}\widetilde{\mathbf{H}}\\ \sqrt{\varepsilon}\widetilde{\mathbf{E}}\end{pmatrix}, \tag{2.4}$$

where

$$\mathbf{D} = \begin{pmatrix}\mathbf{0} & -D_z\otimes I_{N_y}\otimes I_{N_x} & I_{N_z}\otimes D_y\otimes I_{N_x}\\ D_z\otimes I_{N_y}\otimes I_{N_x} & \mathbf{0} & -I_{N_z}\otimes I_{N_y}\otimes D_x\\ -I_{N_z}\otimes D_y\otimes I_{N_x} & I_{N_z}\otimes I_{N_y}\otimes D_x & \mathbf{0}\end{pmatrix}.$$

The initial values of (2.4) are obtained by considering the initial values (1.2) at the collocation points.

2.3. Exact solution in time

In this part, we formulate the exact solution in time of the system (2.4) by using exponential integrators which exactly solve linear systems and also can be used for solving nonlinear systems. This kind of methods has been well researched and has been made successful applications in many systems (see, *e.g.*, [18,21,48,49]). Since the system (2.4) is linear, exponential integrators provide the exact solution. It should be noted that this exact solution suffers from the storage and computation of a $(6N_xN_yN_z) \times (6N_xN_yN_z)$ matrix exponential, which is prohibitive from a computational point of view in many cases. In order to make the computation of the matrix exponential be achievable and effective, matrix diagonalisation method and vector-valued trigonometric functions are employed in this section.

Denote $\mathcal{F}_{N_w}$ the matrix of Fourier transform coefficients with entries given by $(\mathcal{F}_{N_w})_{j,k} = (e^{2\pi i/N_w})^{-jk}$ and $(\mathcal{F}_{N_w}^{-1})_{j,k} = \frac{1}{N_w}(e^{2\pi i/N_w})^{jk}$. Then it is known that $\mathbf{D} = \mathcal{F}^{-1}\Lambda\mathcal{F}$ with

$$\mathcal{F} = \mathrm{diag}\big(\mathcal{F}_{N_z}\otimes\mathcal{F}_{N_y}\otimes\mathcal{F}_{N_x},\mathcal{F}_{N_z}\otimes\mathcal{F}_{N_y}\otimes\mathcal{F}_{N_x},\mathcal{F}_{N_z}\otimes\mathcal{F}_{N_y}\otimes\mathcal{F}_{N_x}\big),$$

$$\Lambda = \begin{pmatrix} \mathbf{0} & -\Lambda_z \otimes I_{N_y} \otimes I_{N_x} & I_{N_z} \otimes \Lambda_y \otimes I_{N_x} \\ \Lambda_z \otimes I_{N_y} \otimes I_{N_x} & \mathbf{0} & -I_{N_z} \otimes I_{N_y} \otimes \Lambda_x \\ -I_{N_z} \otimes \Lambda_y \otimes I_{N_x} & I_{N_z} \otimes I_{N_y} \otimes \Lambda_x & \mathbf{0} \end{pmatrix},$$
$$\Lambda_w = i\Omega_w := i\nu_w \mathrm{diag}\Big(0, 1, \ldots, \frac{N_w}{2} - 1, 0, -\frac{N_w}{2} + 1, \ldots, -2, -1\Big),$$

for $w = x, y, z$. Then letting $\widehat{\mathbf{E}} = \mathcal{F}\widetilde{\mathbf{E}}$, $\widehat{\mathbf{H}} = \mathcal{F}\widetilde{\mathbf{H}}$, (2.4) can be reformulated as

$$\frac{\mathrm{d}}{\mathrm{d}t}\begin{pmatrix} \sqrt{\mu}\widehat{\mathbf{H}} \\ \sqrt{\varepsilon}\widehat{\mathbf{E}} \end{pmatrix} = \widehat{\Lambda}\begin{pmatrix} \sqrt{\mu}\widehat{\mathbf{H}} \\ \sqrt{\varepsilon}\widehat{\mathbf{E}} \end{pmatrix}, \tag{2.5}$$

where $\widehat{\Lambda} = \frac{1}{\sqrt{\mu\varepsilon}}\begin{pmatrix} \mathbf{0} & -\Lambda \\ \Lambda & \mathbf{0} \end{pmatrix}$. The exact solution of (2.5) is

$$\begin{pmatrix} \sqrt{\mu}\widehat{\mathbf{H}}(t) \\ \sqrt{\varepsilon}\widehat{\mathbf{E}}(t) \end{pmatrix} = e^{t\widehat{\Lambda}}\begin{pmatrix} \sqrt{\mu}\widehat{\mathbf{H}}(0) \\ \sqrt{\varepsilon}\widehat{\mathbf{E}}(0) \end{pmatrix}.$$

Here we note that $e^{t\widehat{\Lambda}}$ is the exponential of the matrix $t\widehat{\Lambda}$ which is a $6N_S \times 6N_S$ matrix and generates a strongly continuous semigroup. It is clear that $\widehat{\Lambda}$ is a skew-hermitian matrix and thus $\|e^{t\widehat{\Lambda}}\| = 1$.

Now the key step is to compute the matrix exponential $e^{t\widehat{\Lambda}}$. Firstly, according to [1], $e^{t\widehat{\Lambda}}$ can be expressed by some matrix-valued trigonometric functions.

Lemma 2.1 ([1]). *For the matrix exponential, one has*

$$e^{t\widehat{\Lambda}} = \begin{pmatrix} \cos\Big(\frac{t}{\sqrt{\mu\varepsilon}}\Lambda\Big) & -\sin\Big(\frac{t}{\sqrt{\mu\varepsilon}}\Lambda\Big) \\ \sin\Big(\frac{t}{\sqrt{\mu\varepsilon}}\Lambda\Big) & \cos\Big(\frac{t}{\sqrt{\mu\varepsilon}}\Lambda\Big) \end{pmatrix}.$$

Proof. It is easy to see that $\widehat{\Lambda}^k = \frac{1}{(\sqrt{\mu\varepsilon})^k}\begin{pmatrix} \mathbf{0} & -\Lambda^k \\ \Lambda^k & \mathbf{0} \end{pmatrix}$ for $k = 4m+1$, $\frac{1}{(\sqrt{\mu\varepsilon})^k}\begin{pmatrix} -\Lambda^k & \mathbf{0} \\ \mathbf{0} & -\Lambda^k \end{pmatrix}$ for $k = 4m+2$, $\frac{1}{(\sqrt{\mu\varepsilon})^k}\begin{pmatrix} \mathbf{0} & \Lambda^k \\ -\Lambda^k & \mathbf{0} \end{pmatrix}$ for $k = 4m+3$, and $\frac{1}{(\sqrt{\mu\varepsilon})^k}\begin{pmatrix} \Lambda^k & \mathbf{0} \\ \mathbf{0} & \Lambda^k \end{pmatrix}$ for $k = 4m$. Then one gets

$$e^{t\widehat{\Lambda}} = \sum_{k=0}^{\infty}\frac{1}{k!}\widehat{\Lambda}^k = \sum_{m=0}^{\infty}\begin{pmatrix} \frac{\Lambda^{4m}}{(4m)!\left(\sqrt{\mu\varepsilon}\right)^{4m}} - \frac{\Lambda^{4m+2}}{(4m+2)!\left(\sqrt{\mu\varepsilon}\right)^{4m+2}} & -\frac{\Lambda^{4m+1}}{(4m+1)!\left(\sqrt{\mu\varepsilon}\right)^{4m+1}} + \frac{\Lambda^{4m+3}}{(4m+3)!\left(\sqrt{\mu\varepsilon}\right)^{4m+3}} \\ \frac{\Lambda^{4m+1}}{(4m+1)!\left(\sqrt{\mu\varepsilon}\right)^{4m+1}} - \frac{\Lambda^{4m+3}}{(4m+3)!\left(\sqrt{\mu\varepsilon}\right)^{4m+3}} & \frac{\Lambda^{4m}}{(4m)!\left(\sqrt{\mu\varepsilon}\right)^{4m}} - \frac{\Lambda^{4m+2}}{(4m+2)!\left(\sqrt{\mu\varepsilon}\right)^{4m+2}} \end{pmatrix},$$

which confirms the result. □

Based on this result, the next step is to compute the matrix-valued trigonometric functions $\cos(t\Lambda/\sqrt{\mu\varepsilon})$ and $\sin(t\Lambda/\sqrt{\mu\varepsilon})$, which is done by the following proposition.

Proposition 2.2. *It follows that*

$$\cos(t\Lambda/\sqrt{\mu\varepsilon}) = \begin{pmatrix} \boldsymbol{c}_{11}\big(t\Lambda/\sqrt{\mu\varepsilon}\big) & \boldsymbol{c}_{12}\big(t\Lambda/\sqrt{\mu\varepsilon}\big) & \boldsymbol{c}_{13}\big(t\Lambda/\sqrt{\mu\varepsilon}\big) \\ \boldsymbol{c}_{12}\big(t\Lambda/\sqrt{\mu\varepsilon}\big) & \boldsymbol{c}_{22}\big(t\Lambda/\sqrt{\mu\varepsilon}\big) & \boldsymbol{c}_{23}\big(t\Lambda/\sqrt{\mu\varepsilon}\big) \\ \boldsymbol{c}_{13}\big(t\Lambda/\sqrt{\mu\varepsilon}\big) & \boldsymbol{c}_{23}\big(t\Lambda/\sqrt{\mu\varepsilon}\big) & \boldsymbol{c}_{33}\big(t\Lambda/\sqrt{\mu\varepsilon}\big) \end{pmatrix},$$
$$\sin(t\Lambda/\sqrt{\mu\varepsilon}) = \begin{pmatrix} \mathbf{0} & -\boldsymbol{s}_{12}\big(t\Lambda/\sqrt{\mu\varepsilon}\big) & \boldsymbol{s}_{13}\big(t\Lambda/\sqrt{\mu\varepsilon}\big) \\ \boldsymbol{s}_{12}\big(t\Lambda/\sqrt{\mu\varepsilon}\big) & \mathbf{0} & -\boldsymbol{s}_{23}\big(t\Lambda/\sqrt{\mu\varepsilon}\big) \\ -\boldsymbol{s}_{13}\big(t\Lambda/\sqrt{\mu\varepsilon}\big) & \boldsymbol{s}_{23}\big(t\Lambda/\sqrt{\mu\varepsilon}\big) & \mathbf{0} \end{pmatrix},$$

where

$$\begin{aligned}
\boldsymbol{c}_{11}(t\Lambda) &= I + \frac{t^2(\Omega_3^2+\Omega_2^2)\Big(\cos\Big(\sqrt{\Psi(t\Omega)}\Big)-I\Big)}{\Psi(t\Omega)}, \quad \boldsymbol{c}_{12}(t\Lambda) = -\frac{t^2\Omega_2\Omega_1\Big(\cos\Big(\sqrt{\Psi(t\Omega)}\Big)-I\Big)}{\Psi(t\Omega)},\\
\boldsymbol{c}_{22}(t\Lambda) &= I + \frac{t^2(\Omega_3^2+\Omega_1^2)\Big(\cos\Big(\sqrt{\Psi(t\Omega)}\Big)-I\Big)}{\Psi(t\Omega)}, \quad \boldsymbol{c}_{13}(t\Lambda) = -\frac{t^2\Omega_3\Omega_1\Big(\cos\Big(\sqrt{\Psi(t\Omega)}\Big)-I\Big)}{\Psi(t\Omega)},\\
\boldsymbol{c}_{33}(t\Lambda) &= I + \frac{t^2(\Omega_2^2+\Omega_1^2)\Big(\cos\Big(\sqrt{\Psi(t\Omega)}\Big)-I\Big)}{\Psi(t\Omega)}, \quad \boldsymbol{c}_{23}(t\Lambda) = -\frac{t^2\Omega_3\Omega_2\Big(\cos\Big(\sqrt{\Psi(t\Omega)}\Big)-I\Big)}{\Psi(t\Omega)},\\
\boldsymbol{s}_{12}(t\Lambda) &= \frac{it\Omega_3\sin\Big(\sqrt{\Psi(t\Omega)}\Big)}{\sqrt{\Psi(t\Omega)}}, \quad \boldsymbol{s}_{13}(t\Lambda) = \frac{it\Omega_2\sin\Big(\sqrt{\Psi(t\Omega)}\Big)}{\sqrt{\Psi(t\Omega)}}, \quad \boldsymbol{s}_{23}(t\Lambda) = \frac{it\Omega_1\sin\Big(\sqrt{\Psi(t\Omega)}\Big)}{\sqrt{\Psi(t\Omega)}},
\end{aligned} \tag{2.6}$$

with $\Omega_1 = I_{N_z}\otimes I_{N_y}\otimes\Omega_x$, $\Omega_2 = I_{N_z}\otimes\Omega_y\otimes I_{N_x}$, $\Omega_3 = \Omega_z\otimes I_{N_y}\otimes I_{N_x}$, *and* $\Psi(t\Omega) = t^2(\Omega_1^2+\Omega_2^2+\Omega_3^2)$.

Proof. The proof is similar to that of Lemma 2.1 and we skip it for brevity. □

2.4. Fully discrete scheme

We now present the novel fully discrete scheme of the three-dimensional Maxwell's equations (1.1).

Definition 2.3 (Fully discrete scheme)**.** For solving the three-dimensional Maxwell's equations (1.1), the fully discrete scheme is defined as follows.

Step 1: Space step-sizes and collocation points**.** Choose even integers N_x, N_y, N_z to get the space step-sizes $h_x = (x_R - x_L)/N_x$, $h_y = (y_R - y_L)/N_y$, $h_z = (z_R - z_L)/N_z$ and collocation points (x_j, y_k, z_l).

Step 2: Initial values**.** Considering the initial values (1.2) at these collocation points gives $(\mathbf{E}_x^0, \mathbf{E}_y^0, \mathbf{E}_z^0)$ and $(\mathbf{H}_x^0, \mathbf{H}_y^0, \mathbf{H}_z^0)$, for $w = x, y$ or z

$$\begin{aligned}
\mathbf{E}_w^0 = \big(&E_w(x_1,y_1,z_1,0),\ldots,E_w(x_{N_x},y_1,z_1,0),E_w(x_1,y_2,z_1,0),\ldots,\\
&E_w(x_{N_x},y_2,z_1,0),\ldots,E_w(x_1,y_{N_y},z_{N_z},0),\ldots,E_w(x_{N_x},y_{N_y},z_{N_z},0)\big)^{\intercal},\\
\mathbf{H}_w^0 = \big(&H_w(x_1,y_1,z_1,0),\ldots,H_w(x_{N_x},y_1,z_1,0),H_w(x_1,y_2,z_1,0),\ldots,\\
&H_w(x_{N_x},y_2,z_1,0),\ldots,H_w(x_1,y_{N_y},z_{N_z},0),\ldots,H_w(x_{N_x},y_{N_y},z_{N_z},0)\big)^{\intercal}.
\end{aligned} \tag{2.7}$$

Then the initial values for the system (2.5) are given by

$$\widehat{\mathbf{E}}_w^0 = \big(\mathcal{F}_{N_z}\otimes\mathcal{F}_{N_y}\otimes\mathcal{F}_{N_x}\big)\mathbf{E}_w^0, \qquad \widehat{\mathbf{H}}_w^0 = \big(\mathcal{F}_{N_z}\otimes\mathcal{F}_{N_y}\otimes\mathcal{F}_{N_x}\big)\mathbf{H}_w^0. \tag{2.8}$$

Step 3: Exact time computation**.** For solving the three-dimensional Maxwell's equations (1.1) on the time interval $[0, t_{\text{end}}]$, the following computation is considered

$$\begin{aligned}
\sqrt{\mu}\widehat{\mathbf{H}}_x^{t_{\text{end}}} &= \sqrt{\mu}\Big(\mathbf{c}_{11}(t_{\text{end}}\Lambda/\sqrt{\mu\varepsilon})\widehat{\mathbf{H}}_x^0 + \mathbf{c}_{12}(t_{\text{end}}\Lambda/\sqrt{\mu\varepsilon})\widehat{\mathbf{H}}_y^0 + \mathbf{c}_{13}(t_{\text{end}}\Lambda/\sqrt{\mu\varepsilon})\widehat{\mathbf{H}}_z^0\Big)\\
&\quad - \sqrt{\varepsilon}\Big(-\mathbf{s}_{12}(t_{\text{end}}\Lambda/\sqrt{\mu\varepsilon})\widehat{\mathbf{E}}_y^0 + \mathbf{s}_{13}(t_{\text{end}}\Lambda/\sqrt{\mu\varepsilon})\widehat{\mathbf{E}}_z^0\Big),\\
\sqrt{\mu}\widehat{\mathbf{H}}_y^{t_{\text{end}}} &= \sqrt{\mu}\Big(\mathbf{c}_{12}(t_{\text{end}}\Lambda/\sqrt{\mu\varepsilon})\widehat{\mathbf{H}}_x^0 + \mathbf{c}_{22}(t_{\text{end}}\Lambda/\sqrt{\mu\varepsilon})\widehat{\mathbf{H}}_y^0 + \mathbf{c}_{23}(t_{\text{end}}\Lambda/\sqrt{\mu\varepsilon})\widehat{\mathbf{H}}_z^0\Big)\\
&\quad - \sqrt{\varepsilon}\Big(\mathbf{s}_{12}(t_{\text{end}}\Lambda/\sqrt{\mu\varepsilon})\widehat{\mathbf{E}}_x^0 - \mathbf{s}_{23}(t_{\text{end}}\Lambda/\sqrt{\mu\varepsilon})\widehat{\mathbf{E}}_z^0\Big),\\
\sqrt{\mu}\widehat{\mathbf{H}}_z^{t_{\text{end}}} &= \sqrt{\mu}\Big(\mathbf{c}_{13}(t_{\text{end}}\Lambda/\sqrt{\mu\varepsilon})\widehat{\mathbf{H}}_x^0 + \mathbf{c}_{23}(t_{\text{end}}\Lambda/\sqrt{\mu\varepsilon})\widehat{\mathbf{H}}_y^0 + \mathbf{c}_{33}(t_{\text{end}}\Lambda/\sqrt{\mu\varepsilon})\widehat{\mathbf{H}}_z^0\Big)
\end{aligned}$$

$$
\begin{aligned}
&- \sqrt{\varepsilon}\Big(-\mathbf{s}_{13}(t_{\rm end}\Lambda/\sqrt{\mu\varepsilon})\widehat{\mathbf{E}}_x^0 + \mathbf{s}_{23}(t_{\rm end}\Lambda/\sqrt{\mu\varepsilon})\widehat{\mathbf{E}}_y^0\Big),\\
\sqrt{\varepsilon}\widehat{\mathbf{E}}_x^{t_{\rm end}} &= \sqrt{\varepsilon}\Big(\mathbf{c}_{11}(t_{\rm end}\Lambda/\sqrt{\mu\varepsilon})\widehat{\mathbf{E}}_x^0 + \mathbf{c}_{12}(t_{\rm end}\Lambda/\sqrt{\mu\varepsilon})\widehat{\mathbf{E}}_y^0 + \mathbf{c}_{13}(t_{\rm end}\Lambda/\sqrt{\mu\varepsilon})\widehat{\mathbf{E}}_z^0\Big)\\
&\quad + \sqrt{\mu}\Big(-\mathbf{s}_{12}(t_{\rm end}\Lambda/\sqrt{\mu\varepsilon})\widehat{\mathbf{H}}_y^0 + \mathbf{s}_{13}(t_{\rm end}\Lambda/\sqrt{\mu\varepsilon})\widehat{\mathbf{H}}_z^0\Big),\\
\sqrt{\varepsilon}\widehat{\mathbf{E}}_y^{t_{\rm end}} &= \sqrt{\varepsilon}\Big(\mathbf{c}_{12}(t_{\rm end}\Lambda/\sqrt{\mu\varepsilon})\widehat{\mathbf{E}}_x^0 + \mathbf{c}_{22}(t_{\rm end}\Lambda/\sqrt{\mu\varepsilon})\widehat{\mathbf{E}}_y^0 + \mathbf{c}_{23}(t_{\rm end}\Lambda/\sqrt{\mu\varepsilon})\widehat{\mathbf{E}}_z^0\Big)\\
&\quad + \sqrt{\mu}\Big(\mathbf{s}_{12}(t_{\rm end}\Lambda/\sqrt{\mu\varepsilon})\widehat{\mathbf{H}}_x^0 - \mathbf{s}_{23}(t_{\rm end}\Lambda/\sqrt{\mu\varepsilon})\widehat{\mathbf{H}}_z^0\Big),\\
\sqrt{\varepsilon}\widehat{\mathbf{E}}_z^{t_{\rm end}} &= \sqrt{\varepsilon}\Big(\mathbf{c}_{13}(t_{\rm end}\Lambda/\sqrt{\mu\varepsilon})\widehat{\mathbf{E}}_x^0 + \mathbf{c}_{23}(t_{\rm end}\Lambda/\sqrt{\mu\varepsilon})\widehat{\mathbf{E}}_y^0 + \mathbf{c}_{33}(t_{\rm end}\Lambda/\sqrt{\mu\varepsilon})\widehat{\mathbf{E}}_z^0\Big)\\
&\quad + \sqrt{\mu}\Big(-\mathbf{s}_{13}(t_{\rm end}\Lambda/\sqrt{\mu\varepsilon})\widehat{\mathbf{H}}_x^0 + \mathbf{s}_{23}(t_{\rm end}\Lambda/\sqrt{\mu\varepsilon})\widehat{\mathbf{H}}_y^0\Big),
\end{aligned}
$$

where $\mathbf{c}.$ and $\mathbf{s}.$ are determined by (2.6).

Step 4: Final result**.** The final results

$$\mathbf{E}_w^{t_{\rm end}} \approx (E_w(x_j, y_k, z_l, t_{\rm end}))_{j,k,l} \quad \text{and} \quad \mathbf{H}_w^{t_{\rm end}} \approx (H_w(x_j, y_k, z_l, t_{\rm end}))_{j,k,l}$$

approximating the solution of (1.1) at the collocation points (x_j, y_k, z_l) and at the time $t_{\rm end}$ are given by

$$\mathbf{E}_w^{t_{\rm end}} = \Big(\mathcal{F}_{N_z}^{-1} \otimes \mathcal{F}_{N_y}^{-1} \otimes \mathcal{F}_{N_x}^{-1}\Big)\widehat{\mathbf{E}}_w^{t_{\rm end}}, \quad \mathbf{H}_w^{t_{\rm end}} = \Big(\mathcal{F}_{N_z}^{-1} \otimes \mathcal{F}_{N_y}^{-1} \otimes \mathcal{F}_{N_x}^{-1}\Big)\widehat{\mathbf{H}}_w^{t_{\rm end}}. \tag{2.9}$$

2.5. Fast computation and its cost

In this part, we discuss the complexity of the proposed scheme. A fast solver can be used to increase computational efficiency. The idea is based on the diagonal matrix and the Fast Fourier Transform (FFT) algorithm.

We first discuss the complexity of deriving initial values. Computing the collocation points requires $\mathcal{O}(N_x + N_y + N_z)$ arithmetic operations and storage. Then the storage cost and computational cost of the values $\mathbf{E}_w^0, \mathbf{H}_w^0$ (2.7) are both $\mathcal{O}(N_x N_y N_z)$. The FFT algorithm can be applied to obtain $\widehat{\mathbf{E}}_w^0$, $\widehat{\mathbf{H}}_w^0$ (2.8) and the storage cost is $\mathcal{O}(N_x N_y N_z)$. The details of this procedure and its cost are presented in Algorithm 1.

We then discuss the computational characteristics of the proposed algorithm. We have to compute the coefficients (2.6) and this can be achieved by vector operations since Λ is diagonal. Thus the cost and storage of this step can be reduced to $\mathcal{O}(N_x N_y N_z)$ from $\mathcal{O}(N_x^2 N_y^2 N_z^2)$. Moreover, it is noted here that a great advantage of the scheme is that arbitrary large time step-size is accepted. The final results at any $t_{\rm end}$ are obtained from the initial values by only one step computation with a time step $\triangle t = t_{\rm end}$. Therefore, the cost of the scheme is very low in comparison with the standard methods using a time step-size: $0 < \triangle t < 1$. The detailed complexity of the fully discrete scheme 2.3 is stated in Algorithm 2.

3. Convergence

In this part, we focus on the error estimates of the proposed scheme. For simplicity we consider the cubic domain $\Omega = [0, 2\pi]^3$ with the spatial grid points $N_x = N_y = N_z = N$. A general cuboid domain can be linearly mapped into $\Omega = [0, 2\pi]^3$. Let $C_p^\infty(\Omega)$ be the set of infinitely differentiable periodic functions with period 2π, and $H_p^r(\Omega)$ be the closure of $C_p^\infty(\Omega)$ in $H^r(\Omega)$. Denote the inner product by $\langle u, v\rangle_\Omega = \frac{1}{8\pi^3}\int_\Omega u(x,y,z)\overline{v(x,y,z)}\,{\rm d}x\,{\rm d}y\,{\rm d}z$ whose discrete inner product and norm are given by $\langle u, v\rangle_N = \frac{1}{N^3}\sum_{j=1}^N\sum_{k=1}^N\sum_{l=1}^N u(x_j, y_k, z_l)\overline{v(x_j, y_k, z_l)}$ and $\|u\|_N^2 = \langle u, u\rangle_N$, respectively. Define the norm of

Algorithm 1 (Initial values)**.** The goal of the algorithm is to obtain the initial values $\widehat{\mathbf{E}}_w^0$ and $\widehat{\mathbf{H}}_w^0$ for the method proposed in this paper.

Input N_x, N_y, N_z (even integers)
Output $\widehat{\mathbf{E}}_w^0$, $\widehat{\mathbf{H}}_w^0$ (initial values for our scheme)

1: Compute $h_x = (x_R - x_L)/N_x,\ h_y = (y_R - y_L)/N_y,\ h_z = (z_R - z_L)/N_z$.
Cost: $\mathcal{O}(1)$**. Storage:** $\mathcal{O}(1)$**.**
2: Compute $x_j = x_L + (j-1)h_x,\ y_k = y_L + (k-1)h_y,\ z_l = z_L + (l-1)h_z,\ j = 1, 2, \ldots, N_x,\ k = 1, 2, \ldots, N_y,\ l = 1, 2, \ldots, N_z$.
Cost: $\mathcal{O}(N_x + N_y + N_z)$**. Storage:** $\mathcal{O}(N_x + N_y + N_z)$**.**
3: Compute the values $\mathbf{E}_w^0, \mathbf{H}_w^0$ (2.7) from (1.2) such that

$$[\mathbf{E}_w^0]_{N_xN_y(l-1)+N_x(k-1)+j} = E_w(x_j, y_k, z_l, 0),\quad [\mathbf{H}_w^0]_{N_xN_y(l-1)+N_x(k-1)+j} = H_w(x_j, y_k, z_l, 0)$$

for $w = x, y, z$ and $j = 1, 2, \ldots, N_x,\ k = 1, 2, \ldots, N_y,\ l = 1, 2, \ldots, N_z$.
Cost: $\mathcal{O}\big(N_xN_yN_z\big)$**. Storage:** $\mathcal{O}(N_xN_yN_z)$**.**
4: By Fast Fourier Transform (FFT), compute the initial values

$$\widehat{\mathbf{E}}_w^0 = \big(\mathcal{F}_{N_z} \otimes \mathcal{F}_{N_y} \otimes \mathcal{F}_{N_x}\big)\mathbf{E}_w^0,\qquad \widehat{\mathbf{H}}_w^0 = \big(\mathcal{F}_{N_z} \otimes \mathcal{F}_{N_y} \otimes \mathcal{F}_{N_x}\big)\mathbf{H}_w^0.$$

Cost: $\mathcal{O}(\mathrm{FFT})$**. Storage:** $\mathcal{O}(N_xN_yN_z)$**.**

$H^r(\Omega)$ by $\|\cdot\|_r$ and the seminorm by $|\cdot|_r$. In particular, $\|\cdot\|_0 = \|\cdot\|$. Let the interpolation space

$$\mathcal{S}_N^I = \Bigg\{ u | u = \sum_{|j|,|k|,|l| \le \frac{N}{2}} \frac{\hat{u}_{j,k,l}}{c_j c_k c_l} e^{i(jx+ky+lz)} : \overline{\hat{u}_{j,k,l}} = \hat{u}_{-j,-k,-l}, \hat{u}_{\frac{N}{2},k,l} = \hat{u}_{-\frac{N}{2},k,l},$$
$$\hat{u}_{j,\frac{N}{2},l} = \hat{u}_{j,-\frac{N}{2},l}, \hat{u}_{j,k,\frac{N}{2}} = \hat{u}_{j,k,-\frac{N}{2}} \Bigg\},$$

where $c_l = 1$ for $|l| < \frac{N}{2}$ and $c_l = 2$ for $|l| = \frac{N}{2}$. We denote

$$\mathcal{S}_N^O = \Bigg\{ u | u = \sum_{|j|,|k|,|l| \le \frac{N}{2}} \hat{u}_{j,k,l} e^{i(jx+ky+lz)} : \overline{\hat{u}_{j,k,l}} = \hat{u}_{-j,-k,-l} \Bigg\}.$$

We here remark that $\mathcal{S}_N^I \subseteq \mathcal{S}_N^O$. We denote $\mathcal{P}_N^O : [L^2(\Omega)]^3 \to [\mathcal{S}_N^O]^3$ as the orthogonal projection operator and recall the interpolation operator $\mathcal{P}_N^I : [C(\Omega)]^3 \to [\mathcal{S}_N^I]^3$.

Lemma 3.1 ([3])**.** *For all* $\mathbf{u} \in [\mathcal{S}_N^I]^3$*, we have* $\|\mathbf{u}\|_0 \le \|\mathbf{u}\|_N \le 2\sqrt{2}\|\mathbf{u}\|_0$*. If* $\mathbf{u}, \mathbf{v} \in [\mathcal{S}_N^I]^3$*, then* $\langle \partial_w \mathbf{u}, \mathbf{v}\rangle_N = -\langle \mathbf{u}, \partial_w \mathbf{v}\rangle_N$ *for* $w = x, y, z$*.*

Lemma 3.2 ([3])**.** $\langle \mathcal{P}_N^O \mathbf{u}, \mathbf{v}\rangle_N = \langle \mathbf{u}, \mathbf{v}\rangle_N$ *for* $\mathbf{v} \in [\mathcal{S}_N^O]^3$*. By noting* $\mathcal{P}_N^O \partial_w u = \partial_w \mathcal{P}_N^O u$ *for* $w = x, y, z$*, we can see that* **curl** *and* $\mathcal{P}_N^O$ *satisfy the commutative law.*

Lemma 3.3 ([5])**.** *If* $0 \le \alpha \le r$ *and* $\mathbf{u} \in [H_p^r(\Omega)]^3$*, then* $\|\mathcal{P}_N^O \mathbf{u} - \mathbf{u}\|_\alpha \le CN^{\alpha-r}|\mathbf{u}|_r$ *and in addition if* $r > 3/2$ *then* $\|\mathcal{P}_N^I \mathbf{u} - \mathbf{u}\|_\alpha \le CN^{\alpha-r}|\mathbf{u}|_r$*.*

Theorem 3.4 (Convergence)**.** *Suppose that the exact solution* $\mathbf{H}, \mathbf{E} \in C^1(0, t_{\mathrm{end}}; [H_p^r(\Omega)]^3)$ *and the initial values* $\mathbf{H}_0, \mathbf{E}_0 \in [H_p^r(\Omega)]^3$*, where* $r > 3/2$*, and the initial values are assumed to be bounded. Let* $\mathbf{E}^{t_{\mathrm{end}}} =$

Algorithm 2 (Fully discrete scheme)**.** The goal of the algorithm is to obtain the numerical solution $\mathbf{E}_w^{t_{\rm end}} \in \mathbb{C}^{N_xN_yN_z}$ and $\mathbf{H}_w^{t_{\rm end}} \in \mathbb{C}^{N_xN_yN_z}$ such that $[\mathbf{E}_w^{t_{\rm end}}]_{N_xN_y(l-1)+N_x(k-1)+j} \approx E_w(x_j, y_k, z_l, t_{\rm end})$ and $[\mathbf{H}_w^{t_{\rm end}}]_{N_xN_y(l-1)+N_x(k-1)+j} \approx H_w(x_j, y_k, z_l, t_{\rm end})$ for $w = x, y, z$.

Input $N_x, N_y, N_z, \widehat{\mathbf{E}}_w^0$, $\widehat{\mathbf{H}}_w^0$ (obtained by Algorithm 1) and $t_{\rm end}$

Output $\mathbf{E}_w^{t_{\rm end}}$, $\mathbf{H}_w^{t_{\rm end}}$ (such that $[\mathbf{E}_w^{t_{\rm end}}]_{N_xN_y(l-1)+N_x(k-1)+j} \approx E_w(x_j, y_k, z_l, t_{\rm end})$ and $[\mathbf{H}_w^{t_{\rm end}}]_{N_xN_y(l-1)+N_x(k-1)+j} \approx H_w(x_j, y_k, z_l, t_{\rm end})$)

1: Set $\mathbf{a}_w := \frac{2\pi}{w_R - w_L}(0, 1, \ldots, \frac{N_w}{2} - 1, 0, \frac{N_w}{2} + 1, \ldots, -2, -1)^\intercal \in \mathbb{R}^{N_w}$ for $w = x, y, z$.
Cost: $\mathcal{O}(N_x + N_y + N_z)$**. Storage:** $\mathcal{O}(N_x + N_y + N_z)$**.**

2: Compute $\mathbf{b}_x = \mathbf{1}_{N_z} \otimes \mathbf{1}_{N_y} \otimes \mathbf{a}_x$, $\mathbf{b}_y = \mathbf{1}_{N_z} \otimes \mathbf{a}_y \otimes \mathbf{1}_{N_x}$, $\mathbf{b}_z = \mathbf{a}_z \otimes \mathbf{1}_{N_y} \otimes \mathbf{1}_{N_x}$, and $\Psi = \kappa^2(\mathbf{b}_x^2 + \mathbf{b}_y^2 + \mathbf{b}_z^2)$. Here $\kappa = t_{\rm end}/\sqrt{\mu\varepsilon}$ and $\mathbf{1}_{N_w} = (1, 1, \ldots, 1)^\intercal \in \mathbb{R}^{N_w}$.
Cost: $\mathcal{O}(N_xN_yN_z)$**. Storage:** $\mathcal{O}(N_xN_yN_z)$**.**

3: Compute (**only once**)

$$\mathbf{r}_1 := \Big(\cos\Big(\sqrt{\Psi}\Big) - \mathbf{1}_{N_xN_yN_z}\Big)./\Psi,\ \mathbf{r}_2 := \sin\Big(\sqrt{\Psi}\Big)./\sqrt{\Psi},$$
$$\mathbf{c}_{11} = \mathbf{1}_{N_xN_yN_z} + \kappa^2\big(\mathbf{b}_z^2 + \mathbf{b}_y^2\big).*\mathbf{r}_1,\quad \mathbf{c}_{12} = -\kappa^2\mathbf{b}_y.*\mathbf{b}_x.*\mathbf{r}_1,\quad \mathbf{s}_{12} = i\kappa\mathbf{b}_z.*\mathbf{r}_2,$$
$$\mathbf{c}_{22} = \mathbf{1}_{N_xN_yN_z} + \kappa^2\big(\mathbf{b}_z^2 + \mathbf{b}_x^2\big).*\mathbf{r}_1,\quad \mathbf{c}_{13} = -\kappa^2\mathbf{b}_z.*\mathbf{b}_x.*\mathbf{r}_1,\quad \mathbf{s}_{13} = i\kappa\mathbf{b}_y.*\mathbf{r}_2,$$
$$\mathbf{c}_{33} = \mathbf{1}_{N_xN_yN_z} + \kappa^2\big(\mathbf{b}_y^2 + \mathbf{b}_x^2\big).*\mathbf{r}_1,\quad \mathbf{c}_{23} = -\kappa^2\mathbf{b}_z.*\mathbf{b}_y.*\mathbf{r}_1,\quad \mathbf{s}_{23} = i\kappa\mathbf{b}_x.*\mathbf{r}_2,$$

where ./ and .∗ denote the element-by-element division and multiplication of two vectors, respectively.
Cost: $\mathcal{O}(N_xN_yN_z)$**. Storage:** $\mathcal{O}(N_xN_yN_z)$**.**

4: Compute (**only one step**)

$$\widehat{\mathbf{H}}_x^0 := \sqrt{\mu}\widehat{\mathbf{H}}_x^0,\ \widehat{\mathbf{H}}_y^0 := \sqrt{\mu}\widehat{\mathbf{H}}_y^0,\ \widehat{\mathbf{H}}_z^0 := \sqrt{\mu}\widehat{\mathbf{H}}_z^0,\ \widehat{\mathbf{E}}_x^0 := \sqrt{\varepsilon}\widehat{\mathbf{E}}_x^0,\ \widehat{\mathbf{E}}_y^0 := \sqrt{\varepsilon}\widehat{\mathbf{E}}_y^0,\ \widehat{\mathbf{E}}_z^0 := \sqrt{\varepsilon}\widehat{\mathbf{E}}_z^0,$$
$$\widehat{\mathbf{H}}_x^{t_{\rm end}} = \mathbf{c}_{11}.*\widehat{\mathbf{H}}_x^0 + \mathbf{c}_{12}.*\widehat{\mathbf{H}}_y^0 + \mathbf{c}_{13}.*\widehat{\mathbf{H}}_z^0 + \mathbf{s}_{12}.*\widehat{\mathbf{E}}_y^0 - \mathbf{s}_{13}.*\widehat{\mathbf{E}}_z^0,$$
$$\widehat{\mathbf{H}}_y^{t_{\rm end}} = \mathbf{c}_{12}.*\widehat{\mathbf{H}}_x^0 + \mathbf{c}_{22}.*\widehat{\mathbf{H}}_y^0 + \mathbf{c}_{23}.*\widehat{\mathbf{H}}_z^0 - \mathbf{s}_{12}.*\widehat{\mathbf{E}}_x^0 + \mathbf{s}_{23}.*\widehat{\mathbf{E}}_z^0,$$
$$\widehat{\mathbf{H}}_z^{t_{\rm end}} = \mathbf{c}_{13}.*\widehat{\mathbf{H}}_x^0 + \mathbf{c}_{23}.*\widehat{\mathbf{H}}_y^0 + \mathbf{c}_{33}.*\widehat{\mathbf{H}}_z^0 + \mathbf{s}_{13}.*\widehat{\mathbf{E}}_x^0 - \mathbf{s}_{23}.*\widehat{\mathbf{E}}_y^0,$$
$$\widehat{\mathbf{E}}_x^{t_{\rm end}} = \mathbf{c}_{11}.*\widehat{\mathbf{E}}_x^0 + \mathbf{c}_{12}.*\widehat{\mathbf{E}}_y^0 + \mathbf{c}_{13}.*\widehat{\mathbf{E}}_z^0 - \mathbf{s}_{12}.*\widehat{\mathbf{H}}_y^0 + \mathbf{s}_{13}.*\widehat{\mathbf{H}}_z^0,$$
$$\widehat{\mathbf{E}}_y^{t_{\rm end}} = \mathbf{c}_{12}.*\widehat{\mathbf{E}}_x^0 + \mathbf{c}_{22}.*\widehat{\mathbf{E}}_y^0 + \mathbf{c}_{23}.*\widehat{\mathbf{E}}_z^0 + \mathbf{s}_{12}.*\widehat{\mathbf{H}}_x^0 - \mathbf{s}_{23}.*\widehat{\mathbf{H}}_z^0,$$
$$\widehat{\mathbf{E}}_z^{t_{\rm end}} = \mathbf{c}_{13}.*\widehat{\mathbf{E}}_x^0 + \mathbf{c}_{23}.*\widehat{\mathbf{E}}_y^0 + \mathbf{c}_{33}.*\widehat{\mathbf{E}}_z^0 - \mathbf{s}_{13}.*\widehat{\mathbf{H}}_x^0 + \mathbf{s}_{23}.*\widehat{\mathbf{H}}_y^0,$$
$$\widehat{\mathbf{H}}_x^{t_{\rm end}} := \frac{1}{\sqrt{\mu}}\widehat{\mathbf{H}}_x^{t_{\rm end}},\ \widehat{\mathbf{H}}_y^{t_{\rm end}} := \frac{1}{\sqrt{\mu}}\widehat{\mathbf{H}}_y^{t_{\rm end}},\ \widehat{\mathbf{H}}_z^{t_{\rm end}} := \frac{1}{\sqrt{\mu}}\widehat{\mathbf{H}}_z^{t_{\rm end}},$$
$$\widehat{\mathbf{E}}_x^{t_{\rm end}} := \frac{1}{\sqrt{\varepsilon}}\widehat{\mathbf{E}}_x^{t_{\rm end}},\quad \widehat{\mathbf{E}}_y^{t_{\rm end}} := \frac{1}{\sqrt{\varepsilon}}\widehat{\mathbf{E}}_y^{t_{\rm end}},\quad \widehat{\mathbf{E}}_z^{t_{\rm end}} := \frac{1}{\sqrt{\varepsilon}}\widehat{\mathbf{E}}_z^{t_{\rm end}}.$$

Cost: $\mathcal{O}(N_xN_yN_z)$**. Storage:** $\mathcal{O}(N_xN_yN_z)$**.**

5: Using Inverse Fast Fourier Transform (IFFT), compute for $w = x, y, z$

$$\mathbf{E}_w^{t_{\rm end}} = \Big(\mathcal{F}_{N_z}^{-1} \otimes \mathcal{F}_{N_y}^{-1} \otimes \mathcal{F}_{N_x}^{-1}\Big)\widehat{\mathbf{E}}_w^{t_{\rm end}},\quad \mathbf{H}_w^{t_{\rm end}} = \Big(\mathcal{F}_{N_z}^{-1} \otimes \mathcal{F}_{N_y}^{-1} \otimes \mathcal{F}_{N_x}^{-1}\Big)\widehat{\mathbf{H}}_w^{t_{\rm end}}.$$

Cost: $\mathcal{O}$(IFFT)**. Storage:** $\mathcal{O}(N_xN_yN_z)$**.**

$(\mathbf{E}_x^{t_{\rm end}}, \mathbf{E}_y^{t_{\rm end}}, \mathbf{E}_z^{t_{\rm end}})^\intercal$, $\mathbf{H}^{t_{\rm end}} = (\mathbf{H}_x^{t_{\rm end}}, \mathbf{H}_y^{t_{\rm end}}, \mathbf{H}_z^{t_{\rm end}})^\intercal$ *be the numerical results produced by the scheme 2.3. Then, for any fixed* $t_{\rm end}$*, the error estimate is given by*

$$\Big(\mu\big\|\mathbf{H}^{t_{\rm end}} - \mathbf{H}(t_{\rm end})\big\|_N^2 + \varepsilon\big\|\mathbf{E}^{t_{\rm end}} - \mathbf{E}(t_{\rm end})\big\|_N^2\Big)^{\frac{1}{2}} \le C\big(\sqrt{\mu} + \sqrt{\varepsilon}\big)N^{-r},$$

where $N = N_x = N_y = N_z$ and the constant C is independent of $\Delta t, h_x, h_y, h_z, t_{\rm end}, N, \mu, \varepsilon$.

Proof. Let $\mathbf{E}^* = \mathcal{P}_{N-2}^O \mathbf{E}$, $\mathbf{H}^* = \mathcal{P}_{N-2}^O \mathbf{H}$. The projections of equations (2.1) are written as

$$\frac{\partial}{\partial t}\begin{pmatrix}\sqrt{\mu}\mathbf{H}^*\\ \sqrt{\varepsilon}\mathbf{E}^*\end{pmatrix} = \frac{1}{\sqrt{\mu\varepsilon}}\begin{pmatrix}\mathbf{0} & -\mathbf{curl}\\ \mathbf{curl} & \mathbf{0}\end{pmatrix}\begin{pmatrix}\sqrt{\mu}\mathbf{H}^*\\ \sqrt{\varepsilon}\mathbf{E}^*\end{pmatrix}. \tag{3.1}$$

Noting that $\mathbf{E}^* \in [\mathcal{S}_{N-2}^O]^3 \subseteq [\mathcal{S}_N^I]^3 \subseteq [\mathcal{S}_N^O]^3$, we obtain that

$$\begin{aligned}
\frac{\partial}{\partial x}E_w^*(x_j, y_k, z_l) &= \frac{\partial}{\partial x}\mathcal{P}_N^I E_w^*(x_j, y_k, z_l) = \Big[\mathbf{D}_1 \mathbf{E}_w^*\Big]_{N_xN_y(l-1)+N_x(k-1)+j},\\
\frac{\partial}{\partial y}E_w^*(x_j, y_k, z_l) &= \frac{\partial}{\partial y}\mathcal{P}_N^I E_w^*(x_j, y_k, z_l) = \Big[\mathbf{D}_2 \mathbf{E}_w^*\Big]_{N_xN_y(l-1)+N_x(k-1)+j},\\
\frac{\partial}{\partial z}E_w^*(x_j, y_k, z_l) &= \frac{\partial}{\partial z}\mathcal{P}_N^I E_w^*(x_j, y_k, z_l) = \Big[\mathbf{D}_3 \mathbf{E}_w^*\Big]_{N_xN_y(l-1)+N_x(k-1)+j},
\end{aligned}$$

where $\mathbf{D}_1 = I_{N_z} \otimes I_{N_y} \otimes D_x$, $\mathbf{D}_2 = I_{N_z} \otimes D_y \otimes I_{N_x}$, $\mathbf{D}_3 = D_z \otimes I_{N_y} \otimes I_{N_x}$, and

$$\begin{aligned}
\mathbf{E}_w^* = \Big(&E_{w,1,1,1}^*, E_{w,2,1,1}^*, \ldots, E_{w,N_x,1,1}^*, E_{w,1,2,1}^*, E_{w,2,2,1}^*, \ldots, E_{w,N_x,2,1}^*,\\
&\ldots, E_{w,1,N_y,N_z}^*, E_{w,2,N_y,N_z}^*, \ldots, E_{w,N_x,N_y,N_z}^*\Big)^\intercal \quad \text{for} \quad w = x, y, z.
\end{aligned}$$

Similar results are obvious for $\mathbf{H}^*$. Thus equations (3.1) are transformed into

$$\frac{\mathrm{d}}{\mathrm{d}t}\begin{pmatrix}\sqrt{\mu}\widetilde{\mathbf{H}}^*\\ \sqrt{\varepsilon}\widetilde{\mathbf{E}}^*\end{pmatrix} = \mathcal{D}\begin{pmatrix}\sqrt{\mu}\widetilde{\mathbf{H}}^*\\ \sqrt{\varepsilon}\widetilde{\mathbf{E}}^*\end{pmatrix}, \tag{3.2}$$

with $\mathcal{D} = \frac{1}{\sqrt{\mu\varepsilon}}\begin{pmatrix}\mathbf{0} & -\mathbf{D}\\ \mathbf{D} & \mathbf{0}\end{pmatrix}$ and $\widetilde{\mathbf{H}}^* = (\mathbf{H}_x^*, \mathbf{H}_y^*, \mathbf{H}_z^*)^\intercal$, $\widetilde{\mathbf{E}}^* = (\mathbf{E}_x^*, \mathbf{E}_y^*, \mathbf{E}_z^*)^\intercal$.

On the other hand, the fully discrete scheme (2.3) is equivalent to finding the numerical solution $(\widetilde{\mathbf{H}}, \widetilde{\mathbf{E}})^\intercal \in [\mathcal{S}_N^I]^6$ such that

$$\left\langle \frac{\mathrm{d}}{\mathrm{d}t}\begin{pmatrix}\sqrt{\mu}\widetilde{\mathbf{H}}\\ \sqrt{\varepsilon}\widetilde{\mathbf{E}}\end{pmatrix}, \begin{pmatrix}\boldsymbol{\mu}\\ \boldsymbol{\nu}\end{pmatrix}\right\rangle_N = \left\langle \mathcal{D}\begin{pmatrix}\sqrt{\mu}\widetilde{\mathbf{H}}\\ \sqrt{\varepsilon}\widetilde{\mathbf{E}}\end{pmatrix}, \begin{pmatrix}\boldsymbol{\mu}\\ \boldsymbol{\nu}\end{pmatrix}\right\rangle_N \tag{3.3}$$

for all $(\boldsymbol{\mu}, \boldsymbol{\nu})^\intercal \in [\mathcal{S}_N^I]^6$.

Denote the errors $\mathcal{H}^t = \widetilde{\mathbf{H}}(t) - \mathbf{H}^*(t)$ and $\mathcal{E}^t = \widetilde{\mathbf{E}}(t) - \mathbf{E}^*(t)$. Based on the formulae (3.2) and (3.3), it is clear that

$$\left\langle \frac{\mathrm{d}}{\mathrm{d}t}\begin{pmatrix}\sqrt{\mu}\mathcal{H}^t\\ \sqrt{\varepsilon}\mathcal{E}^t\end{pmatrix}, \begin{pmatrix}\boldsymbol{\mu}\\ \boldsymbol{\nu}\end{pmatrix}\right\rangle_N = \left\langle \mathcal{D}\begin{pmatrix}\sqrt{\mu}\mathcal{H}^t\\ \sqrt{\varepsilon}\mathcal{E}^t\end{pmatrix}, \begin{pmatrix}\boldsymbol{\mu}\\ \boldsymbol{\nu}\end{pmatrix}\right\rangle_N,$$

which is

$$\left\langle \begin{pmatrix}\sqrt{\mu}\mathcal{H}^t\\ \sqrt{\varepsilon}\mathcal{E}^t\end{pmatrix}, \begin{pmatrix}\boldsymbol{\mu}\\ \boldsymbol{\nu}\end{pmatrix}\right\rangle_N = \left\langle e^{\mathcal{D}}\begin{pmatrix}\sqrt{\mu}\mathcal{H}^0\\ \sqrt{\varepsilon}\mathcal{E}^0\end{pmatrix}, \begin{pmatrix}\boldsymbol{\mu}\\ \boldsymbol{\nu}\end{pmatrix}\right\rangle_N.$$

Taking $\begin{pmatrix}\boldsymbol{\mu}\\ \boldsymbol{\nu}\end{pmatrix} = \begin{pmatrix}\sqrt{\mu}\mathcal{H}^t\\ \sqrt{\varepsilon}\mathcal{E}^t\end{pmatrix} + e^{\mathcal{D}}\begin{pmatrix}\sqrt{\mu}\mathcal{H}^0\\ \sqrt{\varepsilon}\mathcal{E}^0\end{pmatrix}$ leads to

$$\begin{aligned}
0 = &\left\|\begin{pmatrix}\sqrt{\mu}\mathcal{H}^t\\ \sqrt{\varepsilon}\mathcal{E}^t\end{pmatrix}\right\|_N^2 - \left\|e^{\mathcal{D}}\begin{pmatrix}\sqrt{\mu}\mathcal{H}^0\\ \sqrt{\varepsilon}\mathcal{E}^0\end{pmatrix}\right\|_N^2 + \left\langle \begin{pmatrix}\sqrt{\mu}\mathcal{H}^t\\ \sqrt{\varepsilon}\mathcal{E}^t\end{pmatrix}, e^{\mathcal{D}}\begin{pmatrix}\sqrt{\mu}\mathcal{H}^0\\ \sqrt{\varepsilon}\mathcal{E}^0\end{pmatrix}\right\rangle_N\\
&- \left\langle e^{\mathcal{D}}\begin{pmatrix}\sqrt{\mu}\mathcal{H}^0\\ \sqrt{\varepsilon}\mathcal{E}^0\end{pmatrix}, \begin{pmatrix}\sqrt{\mu}\mathcal{H}^t\\ \sqrt{\varepsilon}\mathcal{E}^t\end{pmatrix}\right\rangle_N = \left\|\begin{pmatrix}\sqrt{\mu}\mathcal{H}^t\\ \sqrt{\varepsilon}\mathcal{E}^t\end{pmatrix}\right\|_N^2 - \left\|\begin{pmatrix}\sqrt{\mu}\mathcal{H}^0\\ \sqrt{\varepsilon}\mathcal{E}^0\end{pmatrix}\right\|_N^2.
\end{aligned}$$

This shows that $\mu\|\mathcal{H}^t\|_N^2+\varepsilon\|\mathcal{E}^t\|_N^2=\mu\|\mathcal{H}^0\|_N^2+\varepsilon\|\mathcal{E}^0\|_N^2$.

In what follows, we estimate $\|\mathcal{H}^0\|_N^2$ and $\|\mathcal{E}^0\|_N^2$. For $\mathcal{H}^0=\widetilde{\mathbf{H}}(0)-\mathcal{P}_{N-2}^O\mathbf{H}(0)\in[\mathcal{S}_N^I]^3$, we transform the norm by using the result $\|\mathcal{H}_0^0\le\|\mathcal{H}^0\|_N\le 2\sqrt{2}\|\mathcal{H}^0\|_0$ (Lem. 3.1) and then study the boundness of $\|\mathcal{H}^0\|_0$. To this end, we compute

$$\begin{aligned}\big\|\mathcal{H}^0\big\|_0&=\Big\|\widetilde{\mathbf{H}}(0)-\mathcal{P}_{N-2}^O\mathbf{H}(0)\Big\|_0=\big\|\mathcal{P}_N^I(0)\mathbf{H}(0)-\mathcal{P}_{N-2}^O\mathbf{H}(0)\big\|_0\\&\le\big\|\mathcal{P}_N^I(0)\mathbf{H}(0)-\mathbf{H}(0)\big\|_0+\big\|\mathcal{P}_{N-2}^O\mathbf{H}(0)-\mathbf{H}(0)\big\|_0\le CN^{-r}.\end{aligned}$$

Similar result $\big\|\mathcal{E}^0\big\|_N\le 2\sqrt{2}\big\|\mathcal{E}^0\big\|_0\le CN^{-r}$ can be obtained. Therefore, $(\mu\|\mathcal{H}^t\|_N^2+\varepsilon\|\mathcal{E}^t\|_N^2)^{\frac12}\le C\sqrt{\mu+\varepsilon}N^{-r}\le C(\sqrt{\mu}+\sqrt{\varepsilon})N^{-r}$.

With these estimates, we are now in a position to present the error

$$\begin{aligned}&\Big(\mu\big\|\mathbf{H}^{t_{\rm end}}-\mathbf{H}(t_{\rm end})\big\|_N^2+\varepsilon\big\|\mathbf{E}^{t_{\rm end}}-\mathbf{E}(t_{\rm end})\big\|_N^2\Big)^{\frac12}\\&\quad\le\left(\mu\Big\|\widetilde{\mathbf{H}}(t_{\rm end})-\mathbf{H}(t_{\rm end})\Big\|_N^2+\varepsilon\Big\|\widetilde{\mathbf{E}}(t_{\rm end})-\mathbf{E}(t_{\rm end})\Big\|_N^2\right)^{\frac12}\\&\quad\le\Big(\mu\big\|\mathcal{H}^{t_{\rm end}}+\mathcal{P}_{N-2}^O\mathbf{H}(t_{\rm end})-\mathbf{H}(t_{\rm end})\big\|_N^2+\varepsilon\big\|\mathcal{E}^{t_{\rm end}}+\mathcal{P}_{N-2}^O\mathbf{E}(t_{\rm end})-\mathbf{E}(t_{\rm end})\big\|_N^2\Big)^{\frac12}\\&\quad\le\sqrt{\mu}\big\|\mathcal{H}^{t_{\rm end}}+\mathcal{P}_{N-2}^O\mathbf{H}(t_{\rm end})-\mathbf{H}(t_{\rm end})\big\|_N+\sqrt{\varepsilon}\big\|\mathcal{E}^{t_{\rm end}}+\mathcal{P}_{N-2}^O\mathbf{E}(t_{\rm end})-\mathbf{E}(t_{\rm end})\big\|_N\\&\quad\le\sqrt{\mu}\big\|\mathcal{P}_{N-2}^O\mathbf{H}(t_{\rm end})-\mathbf{H}(t_{\rm end})\big\|_N+\sqrt{\varepsilon}\big\|\mathcal{P}_{N-2}^O\mathbf{E}(t_{\rm end})-\mathbf{E}(t_{\rm end})\big\|_N+C\big(\sqrt{\mu}+\sqrt{\varepsilon}\big)N^{-r}\\&\quad\le C\big(\sqrt{\mu}+\sqrt{\varepsilon}\big)N^{-r},\end{aligned}$$

where we have used the boundedness (2.2) of the solution to get

$$\begin{aligned}&\sqrt{\mu}\big\|\mathcal{P}_{N-2}^O\mathbf{H}(t_{\rm end})-\mathbf{H}(t_{\rm end})\big\|_N+\sqrt{\varepsilon}\big\|\mathcal{P}_{N-2}^O\mathbf{E}(t_{\rm end})-\mathbf{E}(t_{\rm end})\big\|_N\\&\quad\le 2\sqrt{2}\big(\sqrt{\mu}\big\|\mathcal{P}_{N-2}^O\mathbf{H}(t_{\rm end})-\mathbf{H}(t_{\rm end})\big\|_0+\sqrt{\varepsilon}\big\|\mathcal{P}_{N-2}^O\mathbf{E}(t_{\rm end})-\mathbf{E}(t_{\rm end})\big\|_0\big)\\&\quad\le C\big(\sqrt{\mu}+\sqrt{\varepsilon}\big)(N-2)^{-r}.\end{aligned}$$

□

Remark 3.5. It is noted that the scheme is of spectral accuracy in space and exact in time. For the Maxwell's equations with enough smoothness solutions, the scheme will converge with infinite-order accuracy.

4. Structure preservation laws

In this section, we rigorously prove the discrete structure preservation laws of the proposed scheme including the energy, helicity, momentum, symplecticity, and divergence-free field conservation laws.

Theorem 4.1 (Energy conservation laws)**.** *The solutions* $\mathbf{E}^{t_{\rm end}},\mathbf{H}^{t_{\rm end}}$ *produced by the fully discrete scheme 2.3 satisfy the discrete energy conservation laws*

$$\mathcal{E}_1^{t_{\rm end}}=\mathcal{E}_1^0,\quad\mathcal{E}_2^{t_{\rm end}}=\mathcal{E}_2^0,\quad\mathcal{E}_3^{t_{\rm end}}=\mathcal{E}_3^0,\quad\mathcal{E}_4^{t_{\rm end}}=\mathcal{E}_4^0,\quad\mathcal{E}_5^{t_{\rm end}}=\mathcal{E}_5^0,\quad\mathcal{E}_6^{t_{\rm end}}=\mathcal{E}_6^0,$$

where

$$\begin{aligned}&\mathcal{E}_1^t=\frac{\mu}{2}\langle\mathbf{H}^t,\mathbf{H}^t\rangle_N+\frac{\varepsilon}{2}\langle\mathbf{E}^t,\mathbf{E}^t\rangle_N,\quad\mathcal{E}_2^t=\frac{\mu}{2}\left\langle\frac{\mathrm{d}}{\mathrm{d}t}\mathbf{H}^t,\frac{\mathrm{d}}{\mathrm{d}t}\mathbf{H}^t\right\rangle_N+\frac{\varepsilon}{2}\left\langle\frac{\mathrm{d}}{\mathrm{d}t}\mathbf{E}^t,\frac{\mathrm{d}}{\mathrm{d}t}\mathbf{E}^t\right\rangle_N,\\&\mathcal{E}_3^t=\frac{\mu}{2}\sum_{w=x,y,z}\langle\mathbf{D}_k\mathbf{H}_w^t,\mathbf{D}_k\mathbf{H}_w^t\rangle_N+\frac{\varepsilon}{2}\sum_{w=x,y,z}\langle\mathbf{D}_k\mathbf{E}_w^t,\mathbf{D}_k\mathbf{E}_w^t\rangle_N\quad\text{for } k=1,2,3,\end{aligned}$$

$$\mathcal{E}_4^t = \frac{\mu}{2}\sum_{w=x,y,z}\left\langle \mathbf{D}_k\frac{\mathrm{d}}{\mathrm{d}t}\mathbf{H}_w^t, \mathbf{D}_k\frac{\mathrm{d}}{\mathrm{d}t}\mathbf{H}_w^t\right\rangle_N + \frac{\varepsilon}{2}\sum_{w=x,y,z}\left\langle \mathbf{D}_k\frac{\mathrm{d}}{\mathrm{d}t}\mathbf{E}_w^t, \mathbf{D}_k\frac{\mathrm{d}}{\mathrm{d}t}\mathbf{E}_w^t\right\rangle_N \quad \text{for } k=1,2,3,$$
$$\mathcal{E}_5^t = \frac{\mu}{2}\sum_{w=x,y,z}\left\langle \mathbf{H}_w^t, \mathbf{D}_k\mathbf{H}_w^t\right\rangle_N + \frac{\varepsilon}{2}\sum_{w=x,y,z}\left\langle \mathbf{E}_w^t, \mathbf{D}_k\mathbf{E}_w^t\right\rangle_N \quad \text{for } k=1,2,3,$$
$$\mathcal{E}_6^t = \frac{\mu}{2}\sum_{w=x,y,z}\left\langle \frac{\mathrm{d}}{\mathrm{d}t}\mathbf{H}_w^t, \mathbf{D}_k\frac{\mathrm{d}}{\mathrm{d}t}\mathbf{H}_w^t\right\rangle_N + \frac{\varepsilon}{2}\sum_{w=x,y,z}\left\langle \frac{\mathrm{d}}{\mathrm{d}t}\mathbf{E}_w^t, \mathbf{D}_k\frac{\mathrm{d}}{\mathrm{d}t}\mathbf{E}_w^t\right\rangle_N \quad \text{for } k=1,2,3,$$

with the inner product $\langle\cdot,\cdot\rangle_N$ *and the notations* $\mathbf{D}_1 = I_{N_z}\otimes I_{N_y}\otimes D_x$, $\mathbf{D}_2 = I_{N_z}\otimes D_y\otimes I_{N_x}$, $\mathbf{D}_3 = D_z\otimes I_{N_y}\otimes I_{N_x}$.

Proof. Based on the formulation of fully discrete scheme 2.3, it is known that $\mathbf{E}^{t_{\text{end}}}$ and $\mathbf{H}^{t_{\text{end}}}$ satisfy

$$\frac{\mathrm{d}}{\mathrm{d}t}\begin{pmatrix}\sqrt{\mu}\mathbf{H}^{t_{\text{end}}}\\ \sqrt{\varepsilon}\mathbf{E}^{t_{\text{end}}}\end{pmatrix} = \mathcal{D}\begin{pmatrix}\sqrt{\mu}\mathbf{H}^{t_{\text{end}}}\\ \sqrt{\varepsilon}\mathbf{E}^{t_{\text{end}}}\end{pmatrix}. \tag{4.1}$$

Therefore, we have that

$$\frac{\mathrm{d}}{\mathrm{d}t}\mathcal{E}_1^{t_{\text{end}}} = \mu\big(\mathbf{H}^{t_{\text{end}}}\big)^{\intercal}\dot{\mathbf{H}}^{t_{\text{end}}} + \varepsilon\big(\mathbf{E}^{t_{\text{end}}}\big)^{\intercal}\dot{\mathbf{E}}^{t_{\text{end}}} = \big(\mathbf{H}^{t_{\text{end}}}\big)^{\intercal}\big(-\mathbf{D}\mathbf{E}^{t_{\text{end}}}\big) + \big(\mathbf{E}^{t_{\text{end}}}\big)^{\intercal}\big(\mathbf{D}\mathbf{H}^{t_{\text{end}}}\big).$$

Using the property that $\mathbf{D}^{\intercal} = \mathbf{D}$, one gets

$$\begin{aligned}\frac{\mathrm{d}}{\mathrm{d}t}\mathcal{E}_1^{t_{\text{end}}} &= \big(\mathbf{H}^{t_{\text{end}}}\big)^{\intercal}\big(-\mathbf{D}\mathbf{E}^{t_{\text{end}}}\big) + \Big(\big(\mathbf{E}^{t_{\text{end}}}\big)^{\intercal}\big(\mathbf{D}\mathbf{H}^{t_{\text{end}}}\big)\Big)^{\intercal}\\ &= \big(\mathbf{H}^{t_{\text{end}}}\big)^{\intercal}\big(-\mathbf{D}\mathbf{E}^{t_{\text{end}}}\big) + \big(\mathbf{H}^{t_{\text{end}}}\big)^{\intercal}\big(\mathbf{D}\mathbf{E}^{t_{\text{end}}}\big) = 0.\end{aligned}$$

From (4.1), it follows that $\frac{\mathrm{d}^2}{\mathrm{d}t^2}\begin{pmatrix}\sqrt{\mu}\mathbf{H}^{t_{\text{end}}}\\ \sqrt{\varepsilon}\mathbf{E}^{t_{\text{end}}}\end{pmatrix} = \mathcal{D}\frac{\mathrm{d}}{\mathrm{d}t}\begin{pmatrix}\sqrt{\mu}\mathbf{H}^{t_{\text{end}}}\\ \sqrt{\varepsilon}\mathbf{E}^{t_{\text{end}}}\end{pmatrix}$ and hence

$$\begin{aligned}\frac{\mathrm{d}}{\mathrm{d}t}\mathcal{E}_2^{t_{\text{end}}} &= \mu\Big(\dot{\mathbf{H}}^{t_{\text{end}}}\Big)^{\intercal}\ddot{\mathbf{H}}^{t_{\text{end}}} + \varepsilon\Big(\dot{\mathbf{E}}^{t_{\text{end}}}\Big)^{\intercal}\ddot{\mathbf{E}}^{t_{\text{end}}} = \Big(\dot{\mathbf{H}}^{t_{\text{end}}}\Big)^{\intercal}\Big(-\mathbf{D}\dot{\mathbf{E}}^{t_{\text{end}}}\Big) + \Big(\Big(\dot{\mathbf{E}}^{t_{\text{end}}}\Big)^{\intercal}\Big(\mathbf{D}\dot{\mathbf{H}}^{t_{\text{end}}}\Big)\Big)^{\intercal}\\ &= \Big(\dot{\mathbf{H}}^{t_{\text{end}}}\Big)^{\intercal}\Big(-\mathbf{D}\dot{\mathbf{E}}^{t_{\text{end}}}\Big) + \Big(\dot{\mathbf{H}}^{t_{\text{end}}}\Big)^{\intercal}\Big(\mathbf{D}\dot{\mathbf{E}}^{t_{\text{end}}}\Big) = 0.\end{aligned}$$

For the block diagonal matrices $\mathbf{B}_k = \operatorname{diag}(\mathbf{D}_k, \mathbf{D}_k, \mathbf{D}_k)$, it is easy to see that

$$\begin{aligned}\mathbf{B}_k\mathbf{D} &= \begin{pmatrix}\mathbf{D}_k & & \\ & \mathbf{D}_k & \\ & & \mathbf{D}_k\end{pmatrix}\begin{pmatrix}\mathbf{0} & -D_z\otimes I_{N_y}\otimes I_{N_x} & I_{N_z}\otimes D_y\otimes I_{N_x}\\ D_z\otimes I_{N_y}\otimes I_{N_x} & \mathbf{0} & -I_{N_z}\otimes I_{N_y}\otimes D_x\\ -I_{N_z}\otimes D_y\otimes I_{N_x} & I_{N_z}\otimes I_{N_y}\otimes D_x & \mathbf{0}\end{pmatrix}\\ &= \begin{pmatrix}\mathbf{0} & -D_z\otimes I_{N_y}\otimes I_{N_x}\mathbf{D}_k & I_{N_z}\otimes D_y\otimes I_{N_x}\mathbf{D}_k\\ D_z\otimes I_{N_y}\otimes I_{N_x}\mathbf{D}_k & \mathbf{0} & -I_{N_z}\otimes I_{N_y}\otimes D_x\mathbf{D}_k\\ -I_{N_z}\otimes D_y\otimes I_{N_x}\mathbf{D}_k & I_{N_z}\otimes I_{N_y}\otimes D_x\mathbf{D}_k & \mathbf{0}\end{pmatrix} = \mathbf{D}\mathbf{B}_k,\end{aligned}$$

where we have used the commutative law of $\mathbf{D}_k$ which can be shown for $\mathbf{D}_2\mathbf{D}_1$ as follows:

$$\begin{aligned}\mathbf{D}_2\mathbf{D}_1 &= (I_{N_z}\otimes D_y\otimes I_{N_x})\big(I_{N_z}\otimes I_{N_y}\otimes D_x\big)\\ &= I_{N_z}\otimes\big((D_y\otimes I_{N_x})\big(I_{N_y}\otimes D_x\big)\big) = I_{N_z}\otimes D_y\otimes D_x = \mathbf{D}_1\mathbf{D}_2.\end{aligned}$$

Then, left-multiplying (4.1) with block diagonal matrix $\operatorname{diag}(\mathbf{B}_k, \mathbf{B}_k)$, we have

$$\begin{aligned}\frac{\mathrm{d}}{\mathrm{d}t}\begin{pmatrix}\sqrt{\mu}\mathbf{B}_k\mathbf{H}^{t_{\text{end}}}\\ \sqrt{\varepsilon}\mathbf{B}_k\mathbf{E}^{t_{\text{end}}}\end{pmatrix} &= \frac{1}{\sqrt{\mu\varepsilon}}\begin{pmatrix}\mathbf{0} & -\mathbf{B}_k\mathbf{D}\\ \mathbf{B}_k\mathbf{D} & \mathbf{0}\end{pmatrix}\begin{pmatrix}\sqrt{\mu}\mathbf{H}^{t_{\text{end}}}\\ \sqrt{\varepsilon}\mathbf{E}^{t_{\text{end}}}\end{pmatrix}\\ &= \frac{1}{\sqrt{\mu\varepsilon}}\begin{pmatrix}\mathbf{0} & -\mathbf{D}\\ \mathbf{D} & \mathbf{0}\end{pmatrix}\begin{pmatrix}\sqrt{\mu}\mathbf{B}_k\mathbf{H}^{t_{\text{end}}}\\ \sqrt{\varepsilon}\mathbf{B}_k\mathbf{E}^{t_{\text{end}}}\end{pmatrix}.\end{aligned} \tag{4.2}$$

Based on this scheme and the same arguments as $\mathcal{E}_1^{t_{\text{end}}}$, it is obtained that $\frac{\mathrm{d}}{\mathrm{d}t}\mathcal{E}_3^{t_{\text{end}}} = 0$.

The statement of $\mathcal{E}_4^{t_{\text{end}}}$ can be proved by combining the proofs of $\mathcal{E}_2^{t_{\text{end}}}$ and $\mathcal{E}_3^{t_{\text{end}}}$.

For the energy $\mathcal{E}_5^{t_{\text{end}}}$, it is deduced that

$$\begin{aligned}\frac{\mathrm{d}}{\mathrm{d}t}\mathcal{E}_5^{t_{\text{end}}} &= \mu \sum_{w=x,y,z} \big(\mathbf{H}_w^{t_{\text{end}}}\big)^{\intercal}\mathbf{D}_k\dot{\mathbf{H}}_w^{t_{\text{end}}} + \varepsilon \sum_{w=x,y,z} \big(\mathbf{E}_w^{t_{\text{end}}}\big)^{\intercal}\mathbf{D}_k\dot{\mathbf{E}}_w^{t_{\text{end}}} \\ &= \mu\big(\mathbf{H}^{t_{\text{end}}}\big)^{\intercal}\mathbf{B}_k\dot{\mathbf{H}}^{t_{\text{end}}} + \varepsilon\big(\mathbf{E}^{t_{\text{end}}}\big)^{\intercal}\mathbf{B}_k\dot{\mathbf{E}}^{t_{\text{end}}} \\ &= -\big(\mathbf{H}^{t_{\text{end}}}\big)^{\intercal}\mathbf{D}\mathbf{B}_k\mathbf{E}^{t_{\text{end}}} + \big(\mathbf{E}^{t_{\text{end}}}\big)^{\intercal}\mathbf{D}\mathbf{B}_k\mathbf{H}^{t_{\text{end}}} = 0.\end{aligned}$$

The last result of $\mathcal{E}_6^{t_{\text{end}}}$ can be proved in a similar way to that stated above. □

Remark 4.2. It is noted that the first derivatives of $\mathbf{H}^{t_{\text{end}}}, \mathbf{E}^{t_{\text{end}}}$ are required in the results and they are obtained by

$$\dot{\mathbf{E}}_w^{t_{\text{end}}} = \Big(\mathcal{F}_{N_z}^{-1}\otimes\mathcal{F}_{N_y}^{-1}\otimes\mathcal{F}_{N_x}^{-1}\Big)\dot{\widehat{\mathbf{E}}}_w^{\,t_{\text{end}}}, \quad \dot{\mathbf{H}}_w^{t_{\text{end}}} = \Big(\mathcal{F}_{N_z}^{-1}\otimes\mathcal{F}_{N_y}^{-1}\otimes\mathcal{F}_{N_x}^{-1}\Big)\dot{\widehat{\mathbf{H}}}_w^{\,t_{\text{end}}}, \quad \text{for } w = x, y, z,$$

with

$$\begin{aligned}
\dot{\widehat{\mathbf{H}}}_x^{\,t_{\text{end}}} &= -\frac{i}{\mu}\Big(-\Omega_3\widehat{\mathbf{E}}_y^{t_{\text{end}}} + \Omega_2\widehat{\mathbf{E}}_z^{t_{\text{end}}}\Big), & \dot{\widehat{\mathbf{H}}}_y^{\,t_{\text{end}}} &= -\frac{i}{\mu}\Big(\Omega_3\widehat{\mathbf{E}}_x^{t_{\text{end}}} - \Omega_1\widehat{\mathbf{E}}_z^{t_{\text{end}}}\Big), \\
\dot{\widehat{\mathbf{H}}}_z^{\,t_{\text{end}}} &= -\frac{i}{\mu}\Big(-\Omega_2\widehat{\mathbf{E}}_x^{t_{\text{end}}} + \Omega_1\widehat{\mathbf{E}}_y^{t_{\text{end}}}\Big), & \dot{\widehat{\mathbf{E}}}_x^{\,t_{\text{end}}} &= \frac{i}{\varepsilon}\Big(-\Omega_3\widehat{\mathbf{H}}_y^{t_{\text{end}}} + \Omega_2\widehat{\mathbf{H}}_z^{t_{\text{end}}}\Big), \\
\dot{\widehat{\mathbf{E}}}_y^{\,t_{\text{end}}} &= \frac{i}{\varepsilon}\Big(\Omega_3\widehat{\mathbf{H}}_x^{t_{\text{end}}} - \Omega_1\widehat{\mathbf{H}}_z^{t_{\text{end}}}\Big), & \dot{\widehat{\mathbf{E}}}_z^{\,t_{\text{end}}} &= \frac{i}{\varepsilon}\Big(-\Omega_2\widehat{\mathbf{H}}_x^{t_{\text{end}}} + \Omega_1\widehat{\mathbf{H}}_y^{t_{\text{end}}}\Big).
\end{aligned}$$

On the other hand, these discrete energy conservation laws imply the boundness of the numerical solutions in the L^2 norm. Therefore, the scheme proposed in the paper is unconditionally stable.

Theorem 4.3 (Helicity conservation laws)**.** *For the solutions given by the scheme 2.3, two discrete Helicity conservation laws*

$$\mathcal{H}_1^{t_{\text{end}}} = \mathcal{H}_1^0, \ \mathcal{H}_2^{t_{\text{end}}} = \mathcal{H}_2^0$$

hold, where

$$\mathcal{H}_1^t = \frac{1}{2\varepsilon}\big\langle\mathbf{H}^t, \mathbf{D}\mathbf{H}^t\big\rangle_N + \frac{1}{2\mu}\big\langle\mathbf{E}^t, \mathbf{D}\mathbf{E}^t\big\rangle_N, \quad \mathcal{H}_2^t = \frac{1}{2\varepsilon}\Big\langle\frac{\mathrm{d}}{\mathrm{d}t}\mathbf{H}^t, \mathbf{D}\frac{\mathrm{d}}{\mathrm{d}t}\mathbf{H}^t\Big\rangle_N + \frac{1}{2\mu}\Big\langle\frac{\mathrm{d}}{\mathrm{d}t}\mathbf{E}^t, \mathbf{D}\frac{\mathrm{d}}{\mathrm{d}t}\mathbf{E}^t\Big\rangle_N.$$

Proof. Using (4.1), we arrive at

$$\begin{aligned}\frac{\mathrm{d}}{\mathrm{d}t}\mathcal{H}_1^{t_{\text{end}}} &= \frac{1}{\varepsilon}\big(\mathbf{H}^{t_{\text{end}}}\big)^{\intercal}\mathbf{D}\dot{\mathbf{H}}^{t_{\text{end}}} + \frac{1}{\mu}\big(\mathbf{E}^{t_{\text{end}}}\big)^{\intercal}\mathbf{D}\dot{\mathbf{E}}^{t_{\text{end}}} \\ &= \frac{1}{\varepsilon\mu}\big(\mathbf{H}^{t_{\text{end}}}\big)^{\intercal}\mathbf{D}\big(-\mathbf{D}\mathbf{E}^{t_{\text{end}}}\big) + \frac{1}{\mu\varepsilon}\big(\mathbf{E}^{t_{\text{end}}}\big)^{\intercal}\mathbf{D}\big(\mathbf{D}\mathbf{H}^{t_{\text{end}}}\big) \\ &= -\frac{1}{\varepsilon\mu}\big(\mathbf{H}^{t_{\text{end}}}\big)^{\intercal}\mathbf{D}^2\mathbf{E}^{t_{\text{end}}} + \frac{1}{\mu\varepsilon}\big(\mathbf{E}^{t_{\text{end}}}\big)^{\intercal}\mathbf{D}^2\mathbf{H}^{t_{\text{end}}} = 0.\end{aligned}$$

The second statement can be proved by the similar arguments to $\mathcal{H}_1^{t_{\text{end}}}$. □

Theorem 4.4 (Momentum conservation laws)**.** *The solutions of the scheme 2.3 possess the discrete momentum conservation laws* $\mathcal{M}_1^{t_{\text{end}}} = \mathcal{M}_1^0$, $\mathcal{M}_2^{t_{\text{end}}} = \mathcal{M}_2^0$, *where for* $k = 1, 2, 3$

$$\mathcal{M}_1^t = \big\langle\mathbf{H}^t, \boldsymbol{B}_k\mathbf{E}^t\big\rangle_N, \quad \mathcal{M}_2^t = \big\langle\mathbf{E}^t, \boldsymbol{B}_k\mathbf{H}^t\big\rangle_N \ \text{ with } \ \boldsymbol{B}_k = \operatorname{diag}(\mathbf{D}_k, \mathbf{D}_k, \mathbf{D}_k).$$

Proof. We first compute

$$\frac{\mathrm{d}}{\mathrm{d}t}\mathcal{M}_1^{t_{\mathrm{end}}} = \big(\mathbf{H}^{t_{\mathrm{end}}}\big)^{\intercal}\mathbf{B}_k\dot{\mathbf{E}}^{t_{\mathrm{end}}} + \Big(\dot{\mathbf{H}}^{t_{\mathrm{end}}}\Big)^{\intercal}\mathbf{B}_k\mathbf{E}^{t_{\mathrm{end}}} = \frac{1}{\varepsilon}\big(\mathbf{H}^{t_{\mathrm{end}}}\big)^{\intercal}\mathbf{B}_k\mathbf{D}\mathbf{H}^{t_{\mathrm{end}}} - \frac{1}{\mu}\big(\mathbf{D}\mathbf{E}^{t_{\mathrm{end}}}\big)^{\intercal}\mathbf{B}_k\mathbf{E}^{t_{\mathrm{end}}}.$$

With the properties $\mathbf{D}^{\intercal} = \mathbf{D}$, $\mathbf{B}_k^{\intercal} = -\mathbf{B}_k$ and $\mathbf{B}_k\mathbf{D} = \mathbf{D}\mathbf{B}_k$, one has $(\mathbf{B}_k\mathbf{D})^{\intercal} = -\mathbf{B}_k\mathbf{D}$. Thus it is clear that $\frac{\mathrm{d}}{\mathrm{d}t}\mathcal{M}_1^{t_{\mathrm{end}}} = 0$. The other statement can be shown in the same way. □

Theorem 4.5 (Symplecticity conservation law)**.** *The solutions of the scheme 2.3 have the discrete symplecticity conservation law* $d\mathbf{E}^{t_{\mathrm{end}}} \wedge d\mathbf{H}^{t_{\mathrm{end}}} = d\mathbf{E}^0 \wedge d\mathbf{H}^0$, *where*

$$\mathrm{d}\mathbf{E}^t \wedge \mathrm{d}\mathbf{H}^t = \mathrm{d}\mathbf{E}_x^t \wedge \mathrm{d}\mathbf{H}_x^t + \mathrm{d}\mathbf{E}_y^t \wedge \mathrm{d}\mathbf{H}_y^t + \mathrm{d}\mathbf{E}_z^t \wedge \mathrm{d}\mathbf{H}_z^t.$$

Proof. Considering (4.1), we deduce that

$$\begin{pmatrix}\sqrt{\mu}\mathbf{H}^{t_{\mathrm{end}}}\\ \sqrt{\varepsilon}\mathbf{E}^{t_{\mathrm{end}}}\end{pmatrix} = e^{t_{\mathrm{end}}\mathcal{D}}\begin{pmatrix}\sqrt{\mu}\mathbf{H}^0\\ \sqrt{\varepsilon}\mathbf{E}^0\end{pmatrix} = \begin{pmatrix}\cos\Big(\frac{t_{\mathrm{end}}}{\sqrt{\mu\varepsilon}}\mathbf{D}\Big) & -\sin\Big(\frac{t_{\mathrm{end}}}{\sqrt{\mu\varepsilon}}\mathbf{D}\Big)\\ \sin\Big(\frac{t_{\mathrm{end}}}{\sqrt{\mu\varepsilon}}\mathbf{D}\Big) & \cos\Big(\frac{t_{\mathrm{end}}}{\sqrt{\mu\varepsilon}}\mathbf{D}\Big)\end{pmatrix}\begin{pmatrix}\sqrt{\mu}\mathbf{H}^0\\ \sqrt{\varepsilon}\mathbf{E}^0\end{pmatrix}.$$

Therefore, one gets

$$\begin{aligned}\mathrm{d}\mathbf{E}^{t_{\mathrm{end}}} \wedge \mathrm{d}\mathbf{H}^{t_{\mathrm{end}}} &= \frac{1}{\sqrt{\varepsilon}}\mathrm{d}\Big(\sin\Big(\frac{t_{\mathrm{end}}}{\sqrt{\mu\varepsilon}}\mathbf{D}\Big)\sqrt{\mu}\mathbf{H}^0 + \cos\Big(\frac{t_{\mathrm{end}}}{\sqrt{\mu\varepsilon}}\mathbf{D}\Big)\sqrt{\varepsilon}\mathbf{E}^0\Big)\\ &\wedge \frac{1}{\sqrt{\mu}}\mathrm{d}\Big(\cos\Big(\frac{t_{\mathrm{end}}}{\sqrt{\mu\varepsilon}}\mathbf{D}\Big)\sqrt{\mu}\mathbf{H}^0 - \sin\Big(\frac{t_{\mathrm{end}}}{\sqrt{\mu\varepsilon}}\mathbf{D}\Big)\sqrt{\varepsilon}\mathbf{E}^0\Big)\\ &= \cos^2\Big(\frac{t_{\mathrm{end}}}{\sqrt{\mu\varepsilon}}\mathbf{D}\Big)\mathrm{d}\mathbf{E}^0 \wedge \mathrm{d}\mathbf{H}^0 - \sin^2\Big(\frac{t_{\mathrm{end}}}{\sqrt{\mu\varepsilon}}\mathbf{D}\Big)\mathrm{d}\mathbf{H}^0 \wedge \mathrm{d}\mathbf{E}^0 = \mathrm{d}\mathbf{E}^0 \wedge \mathrm{d}\mathbf{H}^0,\end{aligned}$$

where we have used the fact that $\mathrm{d}\mathbf{H}^0 \wedge \mathrm{d}\mathbf{E}^0 = -\mathrm{d}\mathbf{E}^0 \wedge \mathrm{d}\mathbf{H}^0$. □

Theorem 4.6 (Divergence-free field conservation laws)**.** *The following discrete divergence-free field conservation laws hold true for the solutions* $\mathbf{E}^{t_{\mathrm{end}}}, \mathbf{H}^{t_{\mathrm{end}}}$ *produced by the scheme 2.3*

$$\widetilde{\nabla}\cdot\big(\varepsilon\mathbf{E}^{t_{\mathrm{end}}}\big) = \widetilde{\nabla}\cdot\big(\varepsilon\mathbf{E}^0\big), \quad \widetilde{\nabla}\cdot\big(\mu\mathbf{H}^{t_{\mathrm{end}}}\big) = \widetilde{\nabla}\cdot\big(\mu\mathbf{H}^0\big),$$

where $\widetilde{\nabla}\cdot(\varepsilon\mathbf{E}^t) = \mathbf{D}_1(\varepsilon\mathbf{E}_x^t) + \mathbf{D}_2(\varepsilon\mathbf{E}_y^t) + \mathbf{D}_3(\varepsilon\mathbf{E}_z^t)$, $\widetilde{\nabla}\cdot(\mu\mathbf{H}^t) = \mathbf{D}_1(\mu\mathbf{H}_x^t) + \mathbf{D}_2(\mu\mathbf{H}_y^t) + \mathbf{D}_3(\mu\mathbf{H}_z^t)$.

Proof. Concerning the results of $\mathbf{D}_1, \mathbf{D}_2, \mathbf{D}_3$ and $\mathbf{E}^{t_{\mathrm{end}}}$, it can be verified that

$$\begin{aligned}\widetilde{\nabla}\cdot\mathbf{E}^{t_{\mathrm{end}}} &= \mathbf{D}_1\mathbf{E}_x^{t_{\mathrm{end}}} + \mathbf{D}_2\mathbf{E}_y^{t_{\mathrm{end}}} + \mathbf{D}_3\mathbf{E}_z^{t_{\mathrm{end}}}\\ &= \mathcal{F}_{N_S}^{-1}(\Lambda_1\mathbf{c}_{11} + \Lambda_2\mathbf{c}_{12} + \Lambda_3\mathbf{c}_{13})\mathcal{F}_{N_S}\mathbf{E}_x^0 + \mathcal{F}_{N_S}^{-1}(\Lambda_1\mathbf{c}_{12} + \Lambda_2\mathbf{c}_{22} + \Lambda_3\mathbf{c}_{23})\mathcal{F}_{N_S}\mathbf{E}_y^0\\ &\quad + \mathcal{F}_{N_S}^{-1}(\Lambda_1\mathbf{c}_{13} + \Lambda_2\mathbf{c}_{23} + \Lambda_3\mathbf{c}_{33})\mathcal{F}_{N_S}\mathbf{E}_z^0 + \frac{\sqrt{\mu}}{\sqrt{\varepsilon}}\mathcal{F}_{N_S}^{-1}(-\Lambda_1\mathbf{s}_{12} + \Lambda_3\mathbf{s}_{23})\mathcal{F}_{N_S}\mathbf{H}_x^0\\ &\quad + \frac{\sqrt{\mu}}{\sqrt{\varepsilon}}\mathcal{F}_{N_S}^{-1}(\Lambda_2\mathbf{s}_{12} - \Lambda_3\mathbf{s}_{13})\mathcal{F}_{N_S}\mathbf{H}_y^0 + + \frac{\sqrt{\mu}}{\sqrt{\varepsilon}}\mathcal{F}_{N_S}^{-1}(\Lambda_1\mathbf{s}_{13} - \Lambda_2\mathbf{s}_{23})\mathcal{F}_{N_S}\mathbf{H}_z^0,\end{aligned}$$

where $\mathcal{F}_{N_S} = \mathcal{F}_{N_z} \otimes \mathcal{F}_{N_y} \otimes \mathcal{F}_{N_x}$ and we omit $(t_{\mathrm{end}}\Lambda/\sqrt{\mu\varepsilon})$ for brevity. According to the results given in the formulation of the method, it can be checked that

$$\begin{aligned}&\Lambda_1\mathbf{c}_{11} + \Lambda_2\mathbf{c}_{12} + \Lambda_3\mathbf{c}_{13} = \mathbf{I}, \quad \Lambda_1\mathbf{c}_{12} + \Lambda_2\mathbf{c}_{22} + \Lambda_3\mathbf{c}_{23} = \mathbf{I},\\ &\Lambda_1\mathbf{c}_{13} + \Lambda_2\mathbf{c}_{23} + \Lambda_3\mathbf{c}_{33} = \mathbf{I}, \quad -\Lambda_1\mathbf{s}_{12} + \Lambda_3\mathbf{s}_{23} = \mathbf{0},\\ &\Lambda_2\mathbf{s}_{12} - \Lambda_3\mathbf{s}_{13} = \mathbf{0}, \qquad\qquad \Lambda_1\mathbf{s}_{13} - \Lambda_2\mathbf{s}_{23} = \mathbf{0},\end{aligned}$$

which lead to the first result of this theorem. The second one can be proved in a similar way. □

Remark 4.7. These conservation laws stated above are established in a discrete form, *i.e.*, those invariants are defined by $\mathbf{H}^t$ and $\mathbf{E}^t$. For the error between the discrete conservations and the exact conservations, it can be obtained by considering the convergence shown in Theorem 3.4, which leads to the estimate $\mathcal{O}(N^{-r})$. For instance, we take the discrete divergence-free field conservation laws and it can be shown that $|\widetilde{\nabla}\cdot(\varepsilon\mathbf{E}^0)-\nabla\cdot(\varepsilon\mathbf{E}^0)|\leq CN^{-r}$.

5. Numerical experiments

In this section, we present numerical experiments to show the performance of our scheme. These two tests are conducted in a sequential program in MATLAB on a laptop ThinkPad X1 Nano (CPU: 11th Gen Intel(R) Core(TM) i7-1160G7 @ 1.20 GHz 2.11 GHz, Memory: 16 GB, Os: Microsoft Windows 11 with 64bit).

5.1. Standing wave solutions

The first test is devoted to the standing wave solutions of Maxwell's equations (1.1) [3,7]

$$\begin{aligned}
E_x &= \frac{k_y-k_z}{\varepsilon\sqrt{\mu}\omega}\cos(\omega\pi t)\cos(k_x\pi x)\sin(k_y\pi y)\sin(k_z\pi z),\\
H_x &= \sin(\omega\pi t)\sin(k_x\pi x)\cos(k_y\pi y)\cos(k_z\pi z),\\
E_y &= \frac{k_z-k_x}{\varepsilon\sqrt{\mu}\omega}\cos(\omega\pi t)\sin(k_x\pi x)\cos(k_y\pi y)\sin(k_z\pi z),\\
H_y &= \sin(\omega\pi t)\cos(k_x\pi x)\sin(k_y\pi y)\cos(k_z\pi z),\\
E_z &= \frac{k_x-k_y}{\varepsilon\sqrt{\mu}\omega}\cos(\omega\pi t)\sin(k_x\pi x)\sin(k_y\pi y)\cos(k_z\pi z),\\
H_z &= \sin(\omega\pi t)\cos(k_x\pi x)\cos(k_y\pi y)\sin(k_z\pi z),
\end{aligned}$$

where $\varepsilon=\mu=1,\ \omega=\sqrt{\frac{k_x^2+k_y^2+k_z^2}{\varepsilon\mu}},\ k_x=1,\ k_y=2,\ k_z=-3$ and $\Omega=[0,2]^3$.

Energy conservation behaviour

In this part, we test the performance of our scheme in the structure preserving laws, which begins with the energy invariants. Define the relative errors in discrete energy invariants $\mathcal{R}(\mathcal{E}_k)=\frac{|\mathcal{E}_k^{t_{\text{end}}}-\mathcal{E}_k^0|}{|\mathcal{E}_k^0|}$ and display the results of our scheme for $k=1,2,3,4$ in Table 1. We note here that the scheme has a similar behaviour for the other two energy invariants $\mathcal{E}_5,\mathcal{E}_6$ and the corresponding results are skipped for brevity. Then we present in Table 2 the relative changes in discrete helicity and momentum invariants $\mathcal{R}(\mathcal{H}_k)=\frac{|\mathcal{H}_k^{t_{\text{end}}}-\mathcal{H}_k^0|}{|\mathcal{H}_k^0|}$ and $\mathcal{R}(\mathcal{M}_k)=\frac{|\mathcal{M}_k^{t_{\text{end}}}-\mathcal{M}_k^0|}{|\mathcal{M}_k^0|}$ for $k=1,2$. Finally, the relative errors in divergence-free field discrete helicity $\mathcal{R}(\mathcal{D}_1)=|\widetilde{\nabla}\cdot(\varepsilon\mathbf{H}^{t_{\text{end}}})|$ and $\mathcal{R}(\mathcal{D}_2)=|\widetilde{\nabla}\cdot(\varepsilon\mathbf{E}^{t_{\text{end}}})|$ are displayed in Table 3. It can be observed from the results that our scheme preserves the invariants exactly since the relative errors are within the roundoff error of the machine, which supports the theoretical analysis proposed in this paper. To show the long time conservation, we plot the errors in discrete energy invariants on $[0,10\,000]$ and the results are shown in Figure 1. It can be seen that our scheme has a persistent conservation over long times.

Accuracy analysis

For this problem, the regularities are infinite so that as shown in Theorem 3.4 the solutions of the schemes converge with infinite-order accuracy both in space and in time. To show this point, two norms $L_\infty=\max\{\max|\mathbf{E}^{t_{\text{end}}}-\mathbf{E}(t_{\text{end}})|,\max|\mathbf{H}^{t_{\text{end}}}-\mathbf{H}(t_{\text{end}})|\}$ and $L_2=(\|\mathbf{E}^{t_{\text{end}}}-\mathbf{E}(t_{\text{end}})\|_N^2+\|\mathbf{H}^{t_{\text{end}}}-\mathbf{H}(t_{\text{end}})\|_N^2)^{\frac{1}{2}}$ are considered which correspond to the maximal and average errors in solution, respectively. The numerical errors as well as the CPU time used in the scheme are listed in Table 4. From the results, it can be observed that our

TABLE 1. The relative errors in discrete energy invariants for Example 1.

Spatial grid points	Time	$\mathcal{R}(\mathcal{E}_1)$	$\mathcal{R}(\mathcal{E}_2)$	$\mathcal{R}(\mathcal{E}_3)$	$\mathcal{R}(\mathcal{E}_4)$
$N_x = N_y = N_z = 8$	$t_{\text{end}} = 1$	2.9605e−16	2.7425e−16	2.1331e−16	0.0000e−16
	$t_{\text{end}} = 5$	1.4802e−16	1.3712e−16	2.1331e−16	3.9521e−16
	$t_{\text{end}} = 10$	5.9211e−16	4.1138e−16	4.2662e−16	5.9281e−16
	$t_{\text{end}} = 15$	1.4802e−16	1.3712e−16	0.0000e−16	1.9760e−16
	$t_{\text{end}} = 20$	2.9605e−16	4.1138e−16	4.2662e−16	1.9760e−16
$N_x = N_y = N_z = 16$	$t_{\text{end}} = 1$	2.9605e−16	2.7425e−16	2.1331e−16	0.0000e−16
	$t_{\text{end}} = 5$	0.0000e−16	1.3712e−16	4.2662e−16	1.9760e−16
	$t_{\text{end}} = 10$	2.9605e−16	4.1138e−16	4.2662e−16	3.9521e−16
	$t_{\text{end}} = 15$	0.0000e−16	0.0000e−16	0.0000e−16	0.0000e−16
	$t_{\text{end}} = 20$	1.4802e−16	1.3712e−16	4.2662e−16	1.9760e−16

TABLE 2. The relative errors in discrete helicity and momentum invariants for Example 1.

Spatial grid points	Time	$\mathcal{R}(\mathcal{H}_1)$	$\mathcal{R}(\mathcal{H}_2)$	$\mathcal{R}(\mathcal{M}_1)$	$\mathcal{R}(\mathcal{M}_2)$
$N_x = N_y = N_z = 8$	$t_{\text{end}} = 1$	34575e−14	53756e−14	6.6189e−12	5.7559e−12
	$t_{\text{end}} = 5$	10759e−14	44125e−14	8.2414e−12	7.5206e−12
	$t_{\text{end}} = 10$	53193e−15	31357e−15	2.3899e−12	6.0112e−12
	$t_{\text{end}} = 15$	14507e−14	29453e−14	6.4139e−12	6.6866e−12
	$t_{\text{end}} = 20$	42917e−14	63387e−14	3.7772e−12	2.1877e−11
$N_x = N_y = N_z = 16$	$t_{\text{end}} = 1$	2.0793e−14	1.6924e−13	1.2774e−10	5.0600e−10
	$t_{\text{end}} = 5$	1.3323e−14	1.2081e−13	1.2704e−10	5.6392e−10
	$t_{\text{end}} = 10$	6.1976e−14	1.3128e−13	2.6356e−11	5.8609e−10
	$t_{\text{end}} = 15$	6.4600e−14	1.0865e−13	1.7854e−10	5.4005e−10
	$t_{\text{end}} = 20$	4.8450e−15	2.1487e−13	1.2504e−10	3.4773e−10

TABLE 3. The errors in discrete divergence-free field conservation for Example 1.

	$N_x = N_y = N_z = 8$		$N_x = N_y = N_z = 16$	
Time	$\mathcal{R}(\mathcal{D}_1)$	$\mathcal{R}(\mathcal{D}_2)$	$\mathcal{R}(\mathcal{D}_1)$	$\mathcal{R}(\mathcal{D}_2)$
$t_{\text{end}} = 1$	2.5121e−15	4.3962e−14	7.1054e−15	1.4210e−14
$t_{\text{end}} = 5$	2.5121e−15	4.3962e−14	1.4210e−14	1.7763e−14
$t_{\text{end}} = 10$	5.0242e−15	4.3962e−14	1.4210e−14	1.3322e−14
$t_{\text{end}} = 15$	2.5121e−15	2.5121e−14	1.0658e−14	1.0658e−14
$t_{\text{end}} = 20$	2.5121e−15	3.7682e−14	1.4210e−14	1.0658e−14

scheme provides numerical results accurate to within machine precision and the computational cost is very low, which demonstrates the effectiveness and efficiency of the new scheme.

5.2. Traveling wave solutions

The second numerical example concerns the Maxwell's equations (1.1) which have traveling wave solutions ($\varepsilon = \mu = 1$) (see [3])

$$E_x = \cos\Big(2\pi(x+y+z) - 2\sqrt{3}\pi t\Big),\ E_y = -2E_x,$$
$$E_z = E_x,\ H_x = \sqrt{3}E_x,\ H_y = 0,\ H_z = -\sqrt{3}E_x,$$

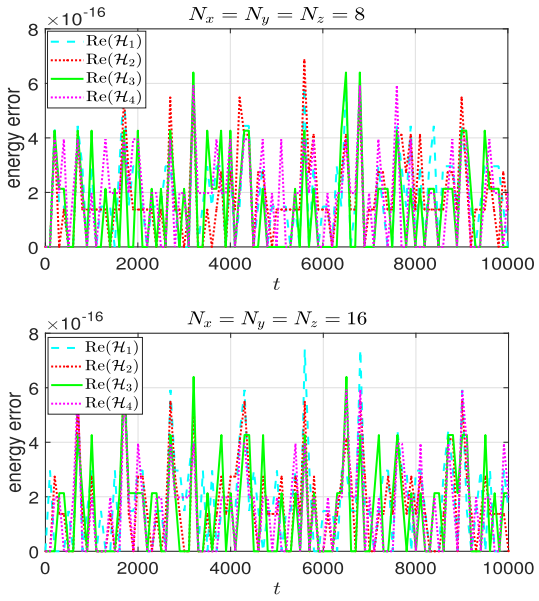

FIGURE 1. Numerical energy conservations of the schemes over long times for Example 1.

TABLE 4. The errors in the solution for Example 1.

	$N_x = N_y = N_z = 8$			$N_x = N_y = N_z = 16$		
Time	L_∞	L_2	CPU (s)	L_∞	L_2	CPU (s)
$t_{\text{end}} = 1$	2.8588e−13	3.6606e−14	0.055	7.0558e−12	3.3915e−13	0.20
$t_{\text{end}} = 5$	7.8246e−13	1.0241e−13	0.023	1.1084e−11	4.4399e−13	0.16
$t_{\text{end}} = 10$	1.4865e−12	1.9932e−13	0.013	1.3474e−11	6.2014e−13	0.16
$t_{\text{end}} = 15$	2.6716e−12	3.9738e−13	0.015	2.1543e−11	1.1193e−12	0.17
$t_{\text{end}} = 20$	2.7995e−12	3.9228e−13	0.030	2.5181e−11	1.2169e−12	0.17

where $t \in [0, t_{\text{end}}]$ and $\Omega = [0, 1]^3$.

Tables 5–7 display the relative errors in discrete energy invariants, discrete helicity and momentum invariants, and discrete divergence-free field conservation, respectively. A long term energy conservation is indicated in Figure 2. The errors in the solution and the corresponding CPU time are listed in Table 8. From the results, it can be observed that our scheme provides a similar numerical phenomena to the first example.

Finally, some numerical comparisons of the existing schemes are made in Table 9, where we choose some methods for comparisons: the structure-preserving method (SAVF(2)) [3], the ADI-FDTD method [55], and the energy conserved splitting FDTD (EC-S-FDTD) method [7]. All these three methods take Fourier pseudospectral method in space and are simulated with $N_x = N_y = N_z = 32$ for solving this numerical test. For the time integrators, SAVF(2) is constructed based on the splitting averaged vector field method, ADI-FDTD considers the finite-difference time-domain method combined with alternating direction implicit technique and EC-S-FDTD uses energy-conserved splitting finite-difference time-domain algorithm. For comparison, our scheme (referred as TEIFP) is implemented with $N_x = N_y = N_z = 16$ and the results clearly show that our scheme has an infinite-order accuracy, which is much better than the existing schemes with finite-order accuracy.

TABLE 5. The relative errors in discrete energy invariants for Example 2.

Spatial grid points	Time	$\mathcal{R}(\mathcal{E}_1)$	$\mathcal{R}(\mathcal{E}_2)$	$\mathcal{R}(\mathcal{E}_3)$	$\mathcal{R}(\mathcal{E}_4)$
$N_x = N_y = N_z = 8$	$t_{\text{end}} = 1$	2.9605e−16	1.5998e−16	1.1998e−16	1.2967e−16
	$t_{\text{end}} = 5$	2.9605e−16	0.0000e−16	1.1998e−16	2.5935e−16
	$t_{\text{end}} = 10$	0.0000e−16	3.1996e−16	3.5996e−16	1.2967e−16
	$t_{\text{end}} = 15$	1.4802e−16	1.5998e−16	1.1998e−16	0.0000e−16
	$t_{\text{end}} = 20$	0.0000e−16	3.1996e−16	1.1998e−16	1.2967e−16
$N_x = N_y = N_z = 16$	$t_{\text{end}} = 1$	0.0000e−16	1.5998e−16	0.0000e−16	0.0000e−16
	$t_{\text{end}} = 5$	2.9605e−16	0.0000e−16	2.3997e−16	0.0000e−16
	$t_{\text{end}} = 10$	1.4802e−16	1.5998e−16	1.1998e−16	2.5935e−16
	$t_{\text{end}} = 15$	2.9605e−16	0.0000e−16	2.3997e−16	1.2967e−16
	$t_{\text{end}} = 20$	1.4802e−16	3.1996e−16	0.0000e−16	2.5935e−16

TABLE 6. The relative errors in discrete helicity and momentum invariants for Example 2.

Spatial grid points	Time	$\mathcal{R}(\mathcal{H}_1)$	$\mathcal{R}(\mathcal{H}_2)$	$\mathcal{R}(\mathcal{M}_1)$	$\mathcal{R}(\mathcal{M}_2)$
$N_x = N_y = N_z = 8$	$t_{\text{end}} = 1$	0.0000e−16	0.0000e−16	0.0000e−16	0.0000e−16
	$t_{\text{end}} = 5$	0.0000e−16	0.0000e−16	0.0000e−16	0.0000e−16
	$t_{\text{end}} = 10$	0.0000e−16	0.0000e−16	0.0000e−16	0.0000e−16
	$t_{\text{end}} = 15$	7.0187e−12	8.3126e−10	2.9103e−16	1.1641e−10
	$t_{\text{end}} = 20$	0.0000e−16	0.0000e−16	0.0000e−16	0.0000e−16
$N_x = N_y = N_z = 16$	$t_{\text{end}} = 1$	0.0000e−16	0.0000e−16	0.0000e−16	0.0000e−16
	$t_{\text{end}} = 5$	0.0000e−16	0.0000e−16	0.0000e−16	0.0000e−16
	$t_{\text{end}} = 10$	3.5454e−9	1.9930e−7	3.7252e−9	3.7252e−9
	$t_{\text{end}} = 15$	2.7610e−9	1.0640e−7	0.0000e−16	7.6798e−9
	$t_{\text{end}} = 20$	5.1680e−9	1.7087e−7	3.7252e−9	8.3300e−9

TABLE 7. The errors in discrete divergence-free field conservation for Example 2.

	$N_x = N_y = N_z = 8$		$N_x = N_y = N_z = 16$	
Time	$\mathcal{R}(\mathcal{D}_1)$	$\mathcal{R}(\mathcal{D}_2)$	$\mathcal{R}(\mathcal{D}_1)$	$\mathcal{R}(\mathcal{D}_2)$
$t_{\text{end}} = 1$	0.0000e−16	0.0000e−16	0.0000e−16	0.0000e−16
$t_{\text{end}} = 5$	0.0000e−16	0.0000e−16	0.0000e−16	0.0000e−16
$t_{\text{end}} = 10$	0.0000e−16	1.0048e−14	0.0000e−16	1.4210e−14
$t_{\text{end}} = 15$	0.0000e−16	1.0048e−14	0.0000e−16	2.8421e−14
$t_{\text{end}} = 20$	0.0000e−16	0.0000e−16	0.0000e−16	1.4210e−14

The numerical results of these two tests highlight the favorable behavior of the scheme presented in this paper. It can be observed that in comparison with other existing structure-preserving methods, the proposed scheme has very high accuracy and exact conservation laws, and requires very low computing cost.

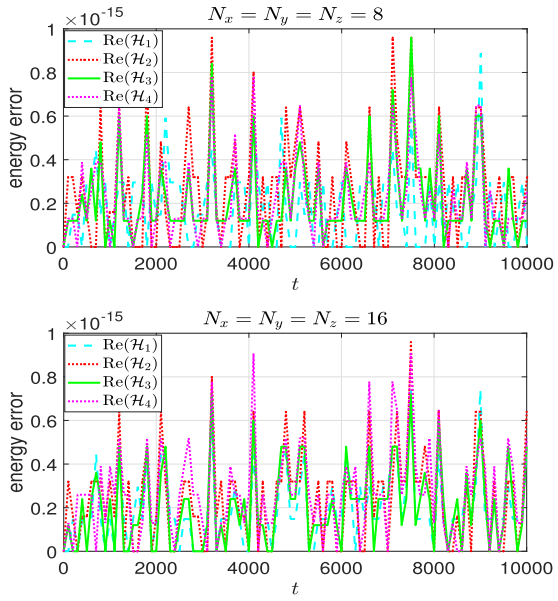

FIGURE 2. Numerical energy conservations of the schemes over long times for Example 2.

TABLE 8. The errors in the solution for Example 2.

	$N_x = N_y = N_z = 8$			$N_x = N_y = N_z = 16$		
Time	L_∞	L_2	CPU (s)	L_∞	L_2	CPU (s)
$t_{\text{end}} = 1$	1.6253e−12	1.5437e−13	0.034	3.5895e−10	7.4340e−12	0.16
$t_{\text{end}} = 5$	6.6265e−12	4.2131e−13	0.013	3.3974e−10	6.7938e−12	0.15
$t_{\text{end}} = 10$	1.4294e−11	8.5423e−13	0.0055	3.9946e−10	7.6605e−12	0.14
$t_{\text{end}} = 15$	3.0699e−12	4.6944e−13	0.0033	2.8697e−10	6.2506e−12	0.14
$t_{\text{end}} = 20$	2.7620e−11	1.6616e−12	0.0061	3.2438e−10	7.6824e−12	0.16

TABLE 9. The errors in the solution for different methods of Example 2.

	$\triangle t = 0.05$		$\triangle t = 0.025$	
Method	L_2	Order	L_2	Order
SAVF(2)	3.74e−2	2.06	9.53e−2	1.97
ADI-FDTD	1.76e−1	1.79	4.53e−2	1.95
EC-S-FDTD	1.41e−1	1.84	3.62e−2	1.96
TEIFP	3.63e−13	Machine accuracy	3.43e−13	Machine accuracy

Acknowledgements

The authors sincerely thank the two anonymous reviewers for the very valuable comments and helpful suggestions. This work was supported by NSFC (12371403, 12271426).

Conflict of Interest

The authors declare that they have no known competing financial interests or personal relationships that could have appeared to influence the work reported in this paper.

References

[1] D.S. Bernstein and W. So, Some explicit formulas for the matrix exponential. *IEEE Trans. Autom. Control* **38** (1993) 1228–1232.

[2] W. Cai, Y. Wang and Y. Song, Numerical dispersion analysis of a multi-symplectic scheme for the three dimensional Maxwell's equations. *J. Comput. Phys.* **234** (2013) 330–352.

[3] J. Cai, J. Hong, Y. Wang and Y. Gong, Two energy-conserved splitting methods for three-dimensional time-domain Maxwell's equations and the convergence analysis. *SIAM. J. Numer. Anal.* **53** (2015) 1918–1940.

[4] J. Cai, J. Hong, Y. Wang and Y. Gong, Numerical analysis of AVF methods for three-dimensional time-domain Maxwell's equations. *J. Sci. Comput.* **66** (2016) 141–176.

[5] C. Canuto and A. Quarteroni, Approximation results for orthogonal polynomials in Sobolev spaces. *Math. Comput.* **38** (1982) 67–86,

[6] W. Chen, X. Li and D. Liang, Energy-conserved splitting FDTD methods for Maxwell's equations. *Numer. Math.* **108** (2008) 445–485.

[7] W. Chen, X. Li and D. Liang, Energy-conserved splitting finite-difference time-domain methods for Maxwell's equations in three dimensions. *SIAM. J. Numer. Anal.* **48** (2010) 1530–1554.

[8] B. Cockburn, F. Li and C.W. Shu, Locally divergence-free discontinuous Galerkin methods for the Maxwell equations. *J. Comput. Phys.* **194** (2004) 588–610.

[9] S. Descombes, S. Lanteri and L. Moya, Locally implicit time integration strategies in a discontinuous Galerkin method for Maxwell's equations. *J. Sci. Comput.* **56** (2013) 190–218.

[10] S. Descombes, S. Lanteri and L. Moya, Locally implicit discontinuous Galerkin time domain method for electromagnetic wave propagation in dispersive media applied to numerical dosimetry in biological tissues. *SIAM J. Sci. Comput.* **38** (2016) A2611–A2633.

[11] R. Diehl, K. Busch and J. Niegemann, Comparison of low-storage Runge–Kutta schemes for discontinuous Galerkin time-domain simulations of Maxwell's equations. *J. Comput. Theo. Nano.* **7** (2010) 1572–1580.

[12] H. Duan, J. Ma and J. Zou, Mixed finite element method with Gauss's law enforced for Maxwell eigenproblem. *SIAM J. Sci. Comput.* **43** (2021) A3677–A3712.

[13] J. Eilinghoff, T. Jahnke and R. Schnaubelt, Error analysis of an energy preserving ADI splitting scheme for the Maxwell equations. *SIAM J. Numer. Anal.* **57** (2019) 1036–1057.

[14] H. Fahs, High-order leap-frog based discontinuous Galerkin method for the time-domain Maxwell equations on non-conforming simplicial meshes. *Numer. Math. Theo. Meth. Appl.* **2** (2009) 275–300.

[15] L. Gao, B. Zhang and D. Liang, The splitting finite-difference time-domain methods for Maxwell's equations in two dimensions. *J. Comput. Appl. Math.* **205** (2007) 207–230.

[16] M.J. Grote and T. Mitkova, Explicit local time-stepping methods for Maxwell's equations. *J. Comput. Appl. Math.* **234** (2010) 3283–3302.

[17] E. Hairer, C. Lubich and G. Wanner, Geometric Numerical Integration: Structure-Preserving Algorithms for Ordinary Differential Equations. Springer, Berlin (2006).

[18] E. Hairer, C. Lubich and B. Wang, A filtered Boris algorithm for charged-particle dynamics in a strong magnetic field. *Numer. Math.* **144** (2020) 787–809.

[19] P. Henning, M. Ohlberger and B. Verfürth, A new heterogeneous multiscale method for time-harmonic Maxwell's equations. *SIAM J. Numer. Anal.* **54** (2016) 3493–3522.

[20] T. Hirono, W. Lui, S. Seki and Y. Yoshikuni, A three-dimensional fourth-order finite-difference time-domain scheme using a symplectic integrator propagator. *IEEE Trans. Microwave Theory Tech.* **49** (2001) 1640–1648.

[21] M. Hochbruck and A. Ostermann, Exponential integrators. *Acta Numer.* **19** (2010) 209–286.

[22] M. Hochbruck and T. Pažur, Implicit Runge–Kutta methods and discontinuous Galerkin discretizations for linear Maxwell's equations. *SIAM J. Numer. Anal.* **53** (2015) 485–507.

[23] M. Hochbruck and A. Sturm, Error analysis of a second-order locally implicit method for linear Maxwell's equations. *SIAM J. Numer. Anal.* **54** (2016) 3167–3191.

[24] M. Hochbruck and A. Sturm, Upwind discontinuous Galerkin space discretization and locally implicit time integration for linear Maxwell's equations. *Math. Comput.* **88** (2019) 1121–1153.

[25] M. Hochbruck, T. Jahnke and R. Schnaubelt, Convergence of an ADI splitting for Maxwell's equations. *Numer. Math.* **129** (2015) 535–561.

[26] M. Hochbruck, B. Maier and C. Stohrer, Heterogeneous multiscale method for Maxwell's equations. *Multi. Model. Simul.* **17** (2019) 1147–1171.

[27] J. Hong, L. Ji and L. Kong, Energy-dissipations splitting finite-difference time-domain method for Maxwell equations with perfectly matched layers. *J. Comput. Phys.* **269** (2014) 201–214.

[28] L. Kong, J. Hong and J. Zhang, Splitting multisymplectic integrators for Maxwell's equations. *J. Comput. Phys.* **229** (2010) 4259–4278.

[29] R. Leis, Initial Boundary Value Problems in Mathematical Physics. Wiley, New York (1986).

[30] D. Liang and Q. Yuan, The spatial fourth-order energy-conserved S-FDTD scheme for Maxwell's equations. *J. Comput. Phys.* **243** (2013) 344–364.

[31] Q. Liu, The PSTD algorithm: a time-domain method requiring only two cells per wavelength. *Microw. Opt. Technol. Lett.* **15** (1997) 158–165.

[32] J.E. Marsden and A. Weinstein, The Hamiltonian structure of the Maxwell–Vlasov equations. *Phys. D* **4** (1982) 394–406.

[33] P. Monk, Finite Element Methods for Maxwell's Equations. Clarendon Press, Oxford (2003).

[34] P. Monk and E. Süli, A convergence analysis of Yee's scheme on nonuniform grids. *SIAM J. Numer. Anal.* **31** (1994) 393–412.

[35] L. Moya, Temporal convergence of a locally implicit discontinuous Galerkin method for Maxwell's equations. *ESAIM Math. Model. Numer. Anal.* **46** (2012) 1225–1246.

[36] C.D. Munz, P. Ommes, R. Schneider, E. Sonnendrücker and U. Voß, Divergence correction techinques for Maxwell solvers based on a hyperbolic model. *J. Comput. Phys.* **161** (2000) 484–511.

[37] T. Namiki, A new FDTD algorithm based on alternating direction implicit method. *IEEE Trans. Micro. Theor. Tech.* **47** (1999) 2003–2007.

[38] T. Pažur, *Error analysis of implicit and exponential time integration of linear Maxwell's equations*, Ph.D. thesis. Karlsruhe Institute of Technology (2013). https://publikationen.bibliothek.kit.edu/1000038617.

[39] J. Shang, High-order compact-difference schemes for time-dependent Maxwell equations. *J. Comput. Phys.* **153** (1999) 312–333.

[40] J. Shen, T. Tang and L. Wang, Spectral Methods: Algorithms, Analysis, Applications. Springer, Berlin (2011).

[41] T.W.H. Sheu, Y. Chung, J. Li and Y. Wang, Development of an explicit non-staggered scheme for solving three-dimensional Maxwell's equations. *Comput. Phys. Commun.* **207** (2016) 258–273.

[42] A. Stern, Y. Tong, M. Desbrun and J.E. Marsden, Geometric computational electrodynamics with variational integrators and discrete differential forms, in Geometry, Mechanics, and Dynamics. Springer, New York (2015) 437–475.

[43] H. Su, M. Qin and R. Scherer, A multisymplectic geometry and a multi-symplectic scheme for Maxwell's equations. *Int. J. Pure. Appl. Math.* **34** (2007) 1–17.

[44] Y. Sun and P.S.P. Tse, Symplectic and multi-symplectic numerical methods for Maxwell's equations. *J. Comput. Phys.* **230** (2011) 2076–2094.

[45] A. Taflove and S.C. Hagness, Computational Electrodynamics. Artech House, Boston (2005).

[46] L.N. Trefethen, Spectral Methods in MATLAB. SIAM, Philadelphia (2000).

[47] J.G. Verwer, Component splitting for semi-discrete Maxwell equations. *BIT* **51** (2011) 427–445.

[48] B. Wang and X. Zhao, Error estimates of some splitting schemes for charged-particle dynamics under strong magnetic field. *SIAM J. Numer. Anal.* **59** (2021) 2075–2105.

[49] B. Wang and X. Zhao, Geometric two-scale integrators for highly oscillatory system: uniform accuracy and near conservations. *SIAM J. Numer. Anal.* **61** (2023) 1246–1277.

[50] X. Wu and B. Wang, Geometric Integrators for Differential Equations with Highly Oscillatory Dolutions. Springer Nature Singapore Pvt Ltd. (2021).

[51] H. Yang, X. Zeng and X. Wu, An approach to solving Maxwell's equations in time domain. *J. Math. Anal. Appl.* **518** (2023) 126678.

[52] K.S. Yee, Numerical solution of initial boundary value problems involving Maxwell's equations in isotropic media. *IEEE Trans. Antennas Propag.* **14** (1966) 302–307.

[53] I. Yousept and J. Zou, Edge element method for optimal control of stationary Maxwell system with Gauss Law. *SIAM J. Numer. Anal.* **55** (2017) 2787–2810.

[54] S. Zhao and G. Wei, High-order FDTD methods via derivative matching for Maxwell's equations with material interfaces. *J. Comput. Phys.* **200** (2004) 60–103.

[55] F. Zheng, Z. Chen and J. Zhang, Toward the development of a three-dimensional unconditionally stable finite-difference time-domain method. *IEEE Trans. Micro. Theor. Tech.* **48** (2000) 1550–1558.

[56] H. Zhu, S. Song and Y. Chen, Multi-symplectic wavelet collocation method for Maxwell's equations. *Adv. Appl. Math. Mech.* **3** (2011) 663–688.